

1

2

3 Running head: Functional similarity between ALB3 and ALB4

4

5

6 Corresponding author:

7 Paul Jarvis

8 Department of Plant Sciences

9 University of Oxford

10 South Parks Road

11 Oxford OX1 3RB, UK

12 Tel: +44 (0)1865 275 017

13 Fax: +44 (0)1865 275 074

14 E-mail: [paul.jarvis@plants.ox.ac.uk](mailto:paul.jarvis@plants.ox.ac.uk)

15

16 Research Areas:

17 Biochemistry and Metabolism: Associate Editor Julian Hibberd (Cambridge)

18 Membranes, Transport and Biogenetics: Associate Editor Anna Amtmann (Glasgow)

19

20

21

22

23

24 Genetic and Physical Interaction Studies Reveal Functional  
25 Similarities between ALB3 and ALB4 in *Arabidopsis*

26

27

28 **Raphael Trösch<sup>a,1</sup>, Mats Töpel<sup>a,2</sup>, Úrsula Flores-Pérez<sup>b</sup>, and Paul Jarvis<sup>a,b,\*</sup>**

29

30 <sup>a</sup> Department of Biology, University of Leicester, Leicester LE1 7RH, UK

31 <sup>b</sup> Department of Plant Sciences, University of Oxford, Oxford, OX1 3RB, UK

32

33

34

35 One-sentence summary:

36 The thylakoid membrane protein ALB4 shares functional similarity and physical interactions  
37 with the homologous protein insertase ALB3, despite sequence-level divergence in a critical  
38 C-terminal domain

39

40

41

42 Footnotes:

43

44 Financial source: This investigation was supported by a Gatsby Charitable Foundation  
45 Sainsbury PhD studentship (to RT), grant CTS 12:507 from Carl Tryggers stiftelse (to MT),  
46 Biotechnology and Biological Sciences Research Council (BBSRC) grants BB/D016541/1,  
47 BB/F020325/1, BB/H008039/1, BB/J009369/1 and BB/J017256/1 (to PJ).

48

49 <sup>1</sup> Present address: Department of Biology, University of Kaiserslautern, Erwin-Schrödinger-  
50 Str. 70, 67663 Kaiserslautern, Germany

51 <sup>2</sup> Present address: University of Gothenburg, Department of Biological and Environmental  
52 Sciences, Sweden

53

54 \*Address correspondence to: [paul.jarvis@plants.ox.ac.uk](mailto:paul.jarvis@plants.ox.ac.uk)

55

56   **Abstract**

57   ALB3 is a well-known component of a thylakoid protein targeting complex that interacts  
58   with the chloroplast signal recognition particle (cpSRP) and the cpSRP receptor, cpFtsY. Its  
59   protein-inserting function has been established mainly for light harvesting complex proteins  
60   (LHCPs), which first interact with the unique chloroplast cpSRP43 component and then are  
61   delivered to the ALB3 integrase by a GTP-dependent cpSRP-cpFtsY interaction. In  
62   *Arabidopsis thaliana*, a subsequently discovered ALB3 homologue, ALB4, has been  
63   proposed to be involved not in LHCP targeting but instead in the stabilisation of the ATP  
64   synthase complex. However, here we show that ALB3 and ALB4 share significant functional  
65   overlap, and that both proteins are required for the efficient insertion of cytochrome f and  
66   potentially other subunits of pigment-bearing protein complexes. Genetic and physical  
67   interactions between ALB4 and ALB3, and physical interactions between ALB4 and cpSRP,  
68   suggest that the two ALB proteins may engage similar sets of interactors for their specific  
69   functions. We propose that ALB4 optimizes the insertion of thylakoid proteins by  
70   participating in the ALB3-cpSRP pathway for certain substrates (e.g., cytochrome f and the  
71   Rieske protein). While ALB4 has clearly diverged from ALB3 in relation to the partner-  
72   recruiting C-terminal domain, our analysis suggests that one putative cpSRP-binding motif  
73   has not been entirely lost.

74

75

## 76 Introduction

77 While the machinery responsible for the import of proteins into chloroplasts is largely a  
78 eukaryotic invention, the internal sorting of chloroplast proteins depends on components  
79 derived from the original endosymbiont (Jarvis and Lopez-Juez, 2013). One such component  
80 was revealed through analysis of the albino *alb3* mutant of *Arabidopsis thaliana*, identified  
81 using a *Ds* insertion screen adapted from maize (Long et al., 1993). The mutant was reported  
82 to have white to light-yellow cotyledons and leaves, abnormal chloroplasts, and reduced  
83 levels of chlorophyll (Sundberg et al., 1997). The affected protein, ALB3, is homologous to  
84 the bacterial membrane protein YidC and to the mitochondrial cytochrome c oxidase complex  
85 assembly factor Oxa1, and was shown to be localised in chloroplast thylakoids. Thus, it was  
86 suggested to play a role similar to that of Oxa1 in the assembly of thylakoid membrane  
87 complexes (Sundberg et al., 1997). Since ALB3 antibodies could inhibit the insertion of  
88 LHCP proteins, the affected thylakoid membrane complexes were identified to be the light  
89 harvesting complexes (Moore et al., 2000). The YidC/Oxa1/Alb3 family of proteins are now  
90 widely recognized to have conserved functions in most organisms, from bacteria to plants,  
91 and are generally involved in the insertion of proteins into membranes, the folding of  
92 membrane proteins, and the assembly of membrane protein complexes (Zhang et al., 2009;  
93 Saller et al., 2012; Dalbey et al., 2014).

94 For the *in vitro* reconstitution of LHCP proteins into thylakoid membranes, it was  
95 previously found that the stroma could be replaced by the chloroplast signal recognition  
96 particle (cpSRP), the cpSRP receptor cpFtsY, and GTP (Tu et al., 1999). The necessity of  
97 ALB3 for LHCP insertion suggested that these stromal factors can deliver LHCPs to the  
98 thylakoids via an interaction with ALB3 at the thylakoid membrane (Moore et al., 2000). The  
99 chloroplast SRP is a heterodimer of cpSRP54 and cpSRP43 in *Arabidopsis* (Groves et al.,  
100 2001; Stengel et al., 2008). These components interact with each other and with their LHCP  
101 cargo in the stroma (Tu et al., 2000; Jonas-Straube et al., 2001), while cpFtsY is required for  
102 thylakoid docking of the cpSRP-LHCP complex and interacts GTP-dependently with  
103 cpSRP54 (Moore et al., 2003). A conserved membrane insertase function was confirmed for  
104 ALB3 by showing that it could complement a bacterial deletion mutant of YidC and restore  
105 the ability to insert membrane proteins (Jiang et al., 2002).

106 Mutants of Alb3 homologues have been isolated in several distantly related species, and  
107 very similar defects in the accumulation of pigments and in thylakoid organisation have been

reported in every case. In *Chlamydomonas reinhardtii*, the knockout of Alb3.1, one of two paralogues, causes a drastic reduction in both chlorophyll and LHCPs, as in *Arabidopsis* (Bellafiore et al., 2002). In the cyanobacterium *Synechocystis* sp. PCC6803, the knockout of the Alb3 homologue slr1471 also leads to impaired thylakoid organisation, reduced levels of photosynthetic pigments, and consequently reduced photosynthetic performance (Spence et al., 2004).

While the importance of ALB3 for the insertion and assembly of pigment-bearing LHCPs in an evolutionary conserved way seems well established, the contribution of ALB3 to the insertion or assembly of other photosystem proteins or components of other thylakoid complexes is less well understood. In *Arabidopsis*, the insertion of PsbS, PsbX, PsbW and PsbY was unaffected by the blocking of ALB3 with anti-ALB3 antibodies, while in *Chlamydomonas* the knockout of Alb3.1 led to a general reduction of photosystem II (PSII) but left PSI, the cytochrome *b<sub>6</sub>f*-complex, and the ATP synthase complex unaffected (Woolhead et al., 2001; Bellafiore et al., 2002). Interaction studies showed that ALB3 is able to bind to PSII core components and that it is likely involved in the assembly of the PSII core (Ossenbuhl et al., 2004; Pasch et al., 2005), which would explain the reduced level of PSII in the *Chlamydomonas* Alb3.1 knockout (Bellafiore et al., 2002). ALB3 was also shown to interact with the chloroplast cpSecY translocase, and it was suggested that these components act together as a cpSRP-specific translocase (Klostermann et al., 2002); however, as removal of cpSecY (SCY1) did not inhibit ALB3 function, the relevance of this interaction for protein insertion via ALB3 was disputed (Mori et al., 1999; Moore et al., 2003).

In *Arabidopsis*, a homologue of ALB3 exists which is called ALB4 (Gerdes et al., 2006). A knockdown mutant of ALB4 was reported to be visibly normal under standard growth conditions, but to have altered chloroplast ultrastructure; the organelles were more spherical in shape and had deteriorated thylakoid structure (Gerdes et al., 2006). A later study reported a slightly reduced growth rate of the *alb4* knockdown line (Benz et al., 2009). Knockout mutants of *alb4* were shown to have reduced amounts of ATP synthase subunits while transcription of those components was not reduced (Benz et al., 2009). Moreover, larger ATP synthase complexes were decreased in favour of smaller intermediate complexes, and the photophosphorylation capacity of the mutant was consequently reduced, pointing to a role for ALB4 in the stabilisation of ATP synthase intermediates during complex assembly (Benz et al., 2009). Although both ALB4 and ALB3 were localised to the same subfraction of stromal lamellae, gel filtration and co-immunoprecipitation revealed no interaction between

ALB3 and ALB4, while ALB4 clearly interacted with ATP synthase subunits, and ALB3 with cpSecY (Benz et al., 2009). Given the strong difference between the phenotypes of the *Arabidopsis alb3* and *alb4* mutants, preferences of ALB3 for light harvesting complex (LHC) and PSII assembly, and ALB4 for ATP synthase assembly, were proposed. However, the consequences of the loss of both ALB3 and ALB4 had not been investigated. Therefore, to address the possibility that ALB3 and ALB4 share some functions, the *alb3 alb4* double mutant was identified and analysed, and genetic and physical interactions of ALB4 with ALB3 and with other components of the cpSRP-targeting pathway were investigated.





## Results

### Basic molecular and genetic analyses of *Arabidopsis alb* mutants

We wished to gain a better understanding of the *in vivo* role of ALB4, and of its functional relationship with ALB3. For the analysis of *alb4* mutants, the line Salk\_136199 was chosen, which has a T-DNA insertion in the sixth intron (Figure 1A) and was described previously (Gerdes et al., 2006; Benz et al., 2009). This line has been reported to accumulate less than 10% of wild-type levels of ALB4 (Gerdes et al., 2006), and to have a growth retardation defect (Benz et al., 2009). To further investigate this potential growth retardation defect, homozygous *alb4* mutants were grown alongside wild type directly on soil. However, under neither long- nor short-day conditions could a growth retardation defect of *alb4* mutant plants be detected, which is in contrast with the results of Benz et al. (2009) (Figure 1B). Even under various stress conditions, we did not observe significant differences between *alb4* mutant plants and wild type (Supplementary Figure S1). This confirms the earlier finding that this *alb4* mutant line does not have a visible phenotype under normal growth conditions (Gerdes et al., 2006). The expression level of *ALB4* was compared to those of *ALB3* and other components of the cpSRP pathway in order to determine if the large difference between the phenotypes of *alb4* and *alb3* mutants could be due to differential gene expression (Supplementary Figure S2). However, although the expression level of *ALB4* is lower than that of *ALB3*, the difference is not large (ratio of expression levels is ~0.8), and *ALB4* actually has a very similar expression level to *cpFtsY*. The mutants of *cpFtsY*, *cpSRP54* and *cpSRP43* all have pronounced chlorotic phenotypes, but the corresponding gene expression levels are in a similar range to those of *ALB3* and *ALB4*. Thus, the difference in phenotype between the *alb4* and *alb3* mutants is unlikely to be caused by differential expression alone.

To assess the functional relationship between ALB3 and ALB4, the *alb4* mutant was crossed to a heterozygous *alb3* mutant (as the homozygous *alb3* genotype is seedling lethal). An *alb3* line containing a T-DNA insertion in the eighth intron was chosen for this analysis (Figure 1A), which contains a greatly reduced amount of ALB3 protein (Figure 1D; Supplementary Figure S3) and is, like *alb4*, in the Col-0 background. In the resulting F<sub>2</sub> generation, green plants that were homozygous for *alb4* and heterozygous for *alb3* were selected (Figure 1C); the F<sub>3</sub> progeny of these plants segregated a quarter of albino *alb3 alb4* double mutants (Figure 1E), indicating that the double-homozygous mutant genotype is viable. This contrasts with the envelope-localized protein import system for which double

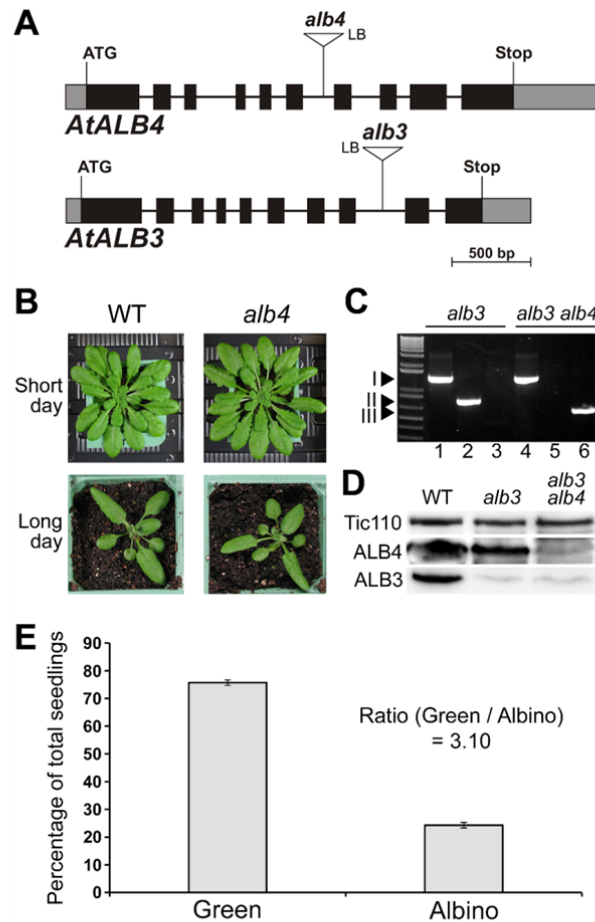


**Figure 1.** Basic characteristics and genetic analysis of the *A. thaliana alb4* and *alb3* mutants. (A) Gene diagrams of *A. thaliana ALB4* and *ALB3* with the T-DNA insertions of the *alb4* and *alb3* mutant lines shown. Protein-coding exons are represented by black boxes, untranslated regions by grey boxes, and introns by thin lines between the boxes. T-DNA insertion sites are indicated precisely, but insertion sizes are not to scale. ATG, translation initiation codon; Stop, translation termination codon; p(A), polyadenylation site; LB, T-DNA left border. (B) Wild-type and *alb4* mutant plants (Salk\_136199) were directly grown on soil under short day (8h light/16h dark) or long day (16h light/8h dark) conditions. Pictures were taken after 7 weeks (Short day) and 4 weeks (Long day). (C) Genotype analysis by genomic PCR. Heterozygous *alb3* mutants (GK\_293B08) and *alb3/+ alb4/alb4* plants were visibly indistinguishable from wild type, but both contained the *alb3* T-DNA insertion (I; lanes 1 and 4); *alb3/+ alb4/alb4* plants additionally contained the homozygous *alb4* T-DNA insertion (III; lanes 3 and 6) but not the wild-type *ALB4* allele (II; lanes 2 and 5). The ladder (lane 0, left side) includes standards of the following sizes, starting at the bottom: 0.3, 0.4, 0.5, 0.65, 0.85, 1.0, 1.65 and 2.0 kb. (D) Immunoblot analysis of total protein extracts from 3-week-old albino plants. The *alb3 alb4* double mutant seedlings contained considerably less ALB4 protein than *alb3* single mutants. (E) Segregation analysis of the progeny of three individual *alb3/+ alb4/alb4* (“het/hom”) plants. Values are means of the percentages of green and albino progeny from each of the three parent plants. The error bars denote standard deviations.

mutants lacking homologous components cause embryo lethality (Constan et al., 2004; Kubis et al., 2004). The identified double-homozygous mutants have a reduced amount of ALB4 protein, as was described earlier for this *alb4* line (Gerdes et al., 2006), and at the same time a greatly reduced amount of ALB3 protein (Figure 1D); the specificity of the ALB3 and ALB4 antibodies used in this and later analyses was tested as shown in Supplementary Figure S3.

188

189 **Double-mutant *alb3 alb4* plants are visibly paler than the *alb3* single mutants with**  
190 **reduced pigment levels**

191 Interestingly, when the double mutants were grown carefully alongside control *alb3* single-  
192 mutant plants, it became clear that the *alb3 alb4* double mutants are visibly paler than the  
193 *alb3* single mutants (Figure 2A). Although the cotyledons did not appear to be significantly  
194 different between the two genotypes, after two weeks growth on medium supplemented with  
195 0.5% sucrose, the first true leaves that emerged from the *alb3* mutant seedlings were  
196 considerably more pigmented (yellowish) than those emerging from the *alb3 alb4* double-  
197 mutant seedlings. The two-week-old seedlings were then transferred onto medium  
198 supplemented with 3% sucrose to support further growth for another week, and the resulting  
199 three-week-old *alb3* seedlings were considerably larger and more yellowish than the *alb3*  
200 *alb4* double-mutant seedlings (Figure 2A). This implies that *alb3* mutants are able to  
201 accumulate photosynthetic pigments more effectively than the *alb3 alb4* double mutants.

202 To directly assess photosynthetic pigment accumulation in the *alb3 alb4* double  
203 mutants, chlorophyll and carotenoids from both genotypes were extracted and quantified.  
204 Significantly, chlorophyll *a* was strongly reduced in the double mutant compared to *alb3*,  
205 while the reduction in chlorophyll *b* was relatively minor (Figure 2B). Thus, the ratio of  
206 chlorophyll *a* to chlorophyll *b* (Chl *a* / Chl *b*) was larger than 2 for *alb3* mutants but smaller  
207 than 1 for *alb3 alb4* double mutants. This is intriguing since chlorophyll *a* binds mainly to  
208 photosynthetic core proteins, suggesting that the predominant loss of chlorophyll *a* in the  
209 *alb3 alb4* double mutants could be caused by a loss of photosynthetic core proteins. In  
210 addition to chlorophyll, the amount of total carotenoids (including carotenes and  
211 xanthophylls) was measured and found to be reduced to approximately one third in the *alb3*  
212 *alb4* double mutants compared to *alb3* single mutants (Figure 2C). The reduction in both  
213 chlorophylls and carotenoids implies that ALB4 is responsible for the accumulation of some  
214 pigment-bearing proteins in the *alb3* background. Severe deficiencies in such proteins in the  
215 *alb3 alb4* double mutants could have a profound effect on the accumulation of thylakoid  
216 membranes, which is examined in detail in the next section.

217

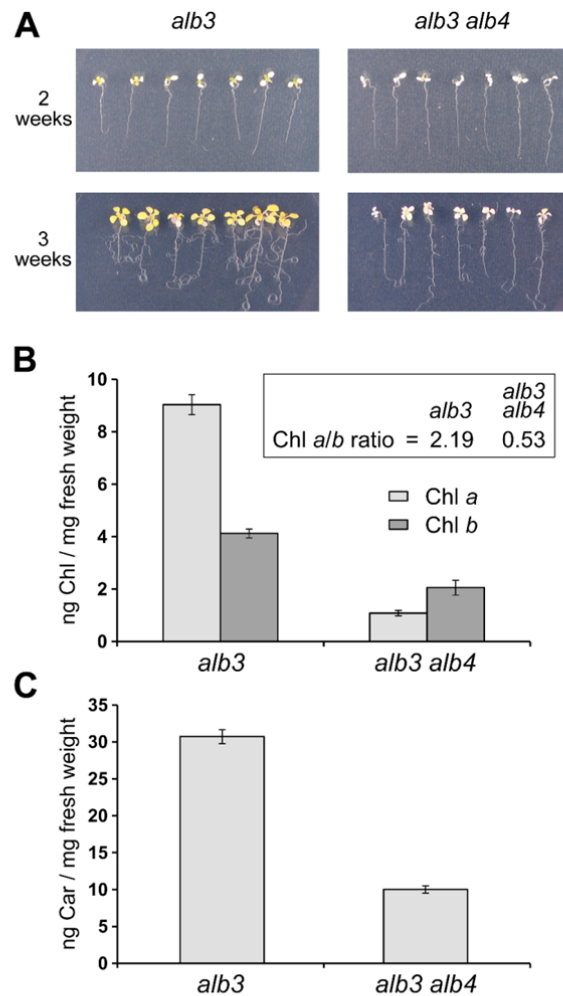


**Figure 2.** Phenotypic analysis of *alb3 alb4* double-mutant plants.

(A) Albino seedlings derived from the segregating progeny of *alb3/+* or *alb3/+ alb4/alb4* plants grown *in vitro* on MS medium supplemented with 0.5% sucrose were transferred to MS medium containing 3% sucrose 2 weeks after germination (upper panels) and allowed to grow on for an additional 1 week (lower panels). (B) Chlorophyll *a* (Chl *a*) and chlorophyll *b* (Chl *b*) were measured in  $\mu\text{g}/\text{mg}$  fresh weight using 3-week-old seedlings grown *in vitro* as described above. The ratio of chlorophyll *a* to chlorophyll *b* (Chl *a*/Chl *b*) is larger than 1 for *alb3* but smaller than 1 for *alb3 alb4*. (C) Total carotenoid (Car) content was measured in  $\mu\text{g}/\text{mg}$  fresh weight using similarly grown 3-week-old seedlings. All error bars denote standard errors ( $n=3$ ).

**The chloroplasts of *alb3 alb4* double mutants have fewer thylakoid membranes than *alb3* chloroplasts**

Plastids lacking ALB3 have been shown previously to form significantly fewer thylakoid membranes than wild type (Sundberg et al., 1997). Here, the mesophyll cell plastids of the first true leaves of 17-day-old seedlings of both *alb3* and *alb3 alb4* double mutants were analysed by transmission electron microscopy. Consistent with the previous report (Sundberg et al., 1997), it was found that *alb3* plastids contain considerably fewer thylakoid membranes, and no granal stacks could be observed (Figure 3A). Interestingly, the *alb3 alb4* double-

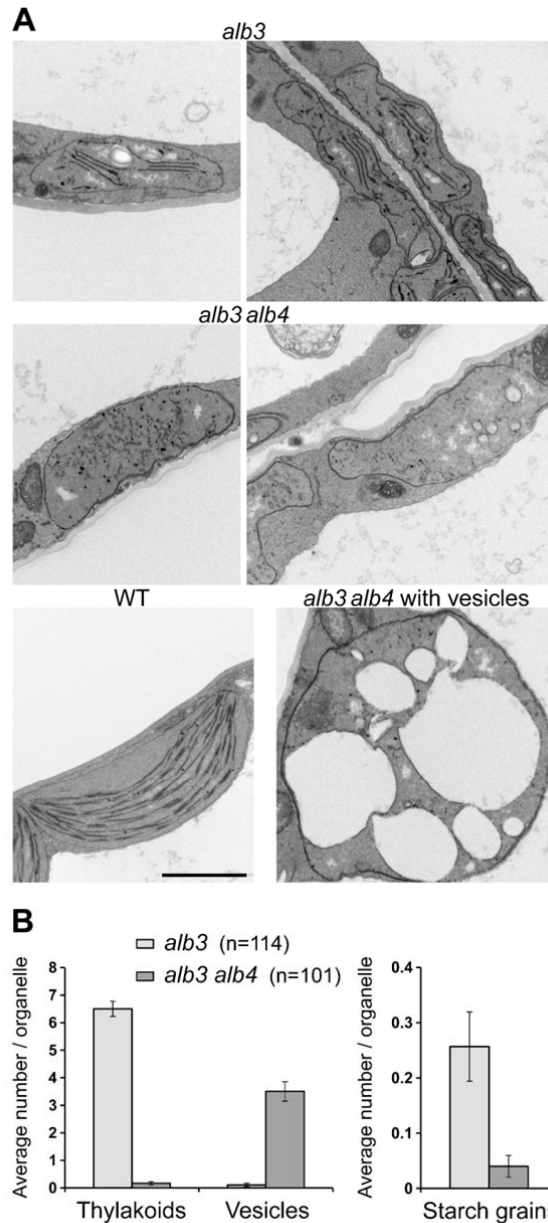


**Figure 3.** Transmission electron micrographs of *alb3* single and *alb3 alb4* double mutants. (A) Transmission electron micrograph images of mesophyll cell plastids from the first true leaves of 17-day-old seedlings grown *in vitro*. All images show plastids at the same scale; the black scale bar in the wild type image corresponds to 2  $\mu$ m. The left image of *alb3* shows a starch grain in the middle of the plastid. The *alb3* plastids generally contain a few thylakoid membranes, while these are lacking almost completely in the *alb3 alb4* double mutants. In the *alb3 alb4* double mutants, large round plastids with many vesicles occur roughly at the same frequency as relatively flat plastids without vesicles. (B) Average number of thylakoids, vesicles and starch grains found in plastids from *alb3* single and *alb3 alb4* double mutants. Numbers in brackets denote total numbers of plastids used for counting. The plastid images analysed were derived from three biological replicates. Error bars denote standard errors (n shown in brackets).

226 mutant plastids were almost completely devoid of thylakoids with many instead accumulating  
 227 large vesicles (Figure 3A), which might be indicative of photooxidative damage (Jakob et al.,  
 228 1997). In the *alb3 alb4* double mutant, large, round plastids containing large vesicles  
 229 occurred with roughly the same frequency as rather flat plastids without vesicles, although

intermediate forms were also present. Generally, the plastids of the *alb3 alb4* double mutant were larger than those of the *alb3* single mutant. Quantification of thylakoid membranes and vesicles in a large number of plastids from both *alb3* single mutants and *alb3 alb4* double mutants showed that *alb3* mutant plastids contain on average 6-7 thylakoids, while thylakoids were virtually absent from *alb3 alb4* double mutants (Figure 3B); on the other hand, *alb3 alb4* double mutants accumulated on average 3-4 large vesicles, while vesicles did not accumulate in *alb3* single mutants. Although it was shown previously that starch grains are absent from *alb3* mutant chloroplasts (Sundberg et al., 1997), some starch grains could be found in a low number of *alb3* mutant chloroplasts (Figure 3B and Figure 3A, top left). However, essentially no starch grains could be observed in the *alb3 alb4* double mutants. This further indicates that the *alb3 alb4* double mutants have a more severe phenotype than the *alb3* single mutants, with reduced photosynthetic capacity, and that therefore there is some functional overlap between ALB3 and ALB4.

#### **ALB4 plays a role in the accumulation of some cytochrome b<sub>6</sub>f components in the thylakoid membranes**

Since *alb3* single mutants accumulate some pigments (of which a large part is chlorophyll *a*) and still contain a few thylakoid membranes, we asked which pigment-binding proteins might be present in the remaining thylakoid membranes in *alb3*. By using western blotting, we found that many photosynthesis-related proteins were already undetectable in the *alb3* single mutant, making it difficult to assess for a role of ALB4 in their assembly by analysis of the double mutant (data not shown). Nonetheless, we found that cytochrome *f* (Cyt *f*) accumulates in the *alb3* mutant but not in the thylakoid-less *alb3 alb4* double mutants (Figure 4, A and C), suggesting that ALB4 alone can insert some Cyt *f* into the remaining thylakoids of *alb3* mutants. Thus, Cyt *f* is a potential client of ALB4. It was shown previously that the cytochrome b<sub>6</sub>f complex contains one molecule of chlorophyll *a* per molecule of Cyt *f* (Dashdorj et al., 2005; Baniulis et al., 2011), and so this complex may be (partly) responsible for the residual pigment-binding activity present in *alb3*. Interestingly, even though the *alb4* single mutant has a wild-type visible phenotype, Cyt *f* is also significantly reduced in *alb4* compared to wild type (Figure 4, B and 4D). This suggests that ALB3 alone cannot efficiently insert Cyt *f*, and that ALB4 plays an important role in the Cyt *f* insertion process.



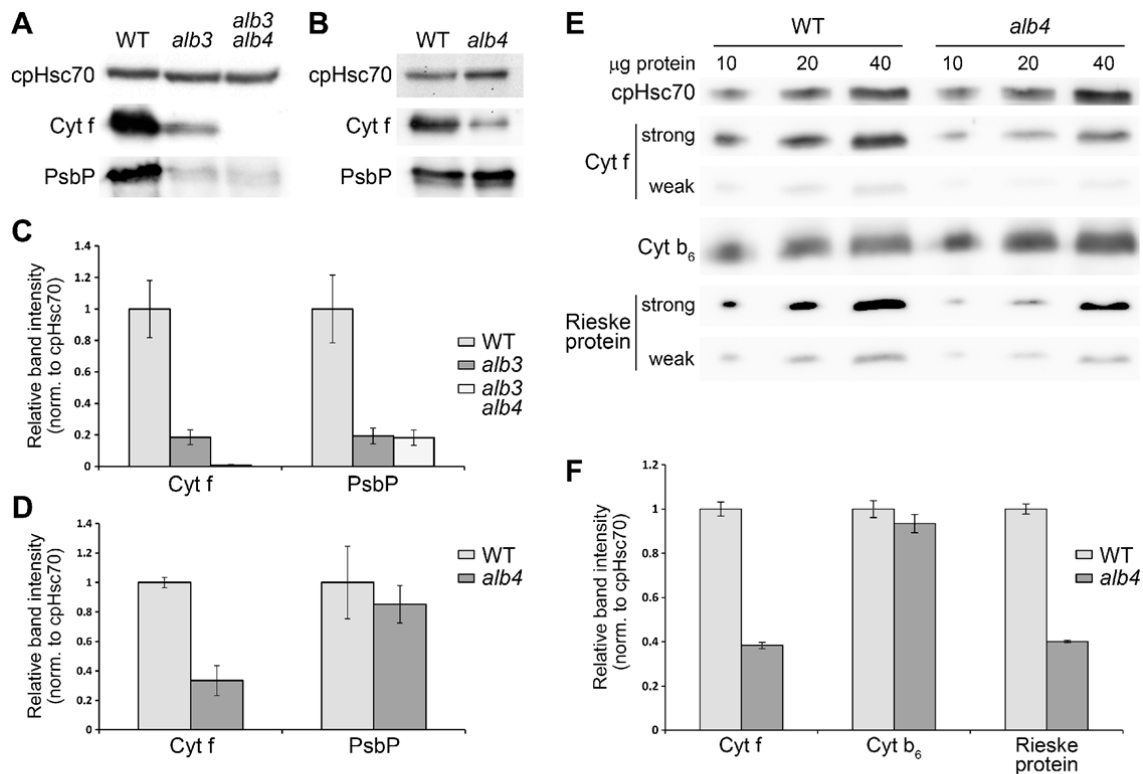


**Figure 4.** Accumulation of thylakoid proteins in *alb3*, *alb4* and double-mutant plants.

(A) Western blot analysis of total protein extracts from 3-week-old seedlings. All seedlings were grown on MS medium containing 0.5% sucrose. The *alb3* and *alb3 alb4* seedlings were transferred to medium containing 3% sucrose at 2 weeks post germination. Sample loading was normalized according to the intensity of the cpHsc70 band. (B) Western blot analysis of total protein extracts from 2-week-old seedlings grown on MS medium containing 0.5% sucrose. (C) Band intensity quantification of the data shown in panel A, normalized according to the cpHsc70 data. Error bars denote standard deviations ( $n=3$ ). The average Cyt f value for wild type has been set to 1. (D) Band intensity quantification of the data shown in panel B, prepared exactly as described for panel C. (E) Western blot analysis of total protein extracts from 2-week-old seedlings grown on MS medium containing 0.5% sucrose. A series of 10, 20 and 40  $\mu$ g of total protein was loaded for each genotype, as indicated. For Cyt f and the Rieske protein, two different exposures are shown (strong and weak), to better illustrate the differences in signal intensity. (F) Band intensity quantification of the data shown in panel E, prepared exactly as described for panel C.

Nevertheless, *alb4* accumulates some Cyt f, suggesting that only the concerted action of ALB3 and ALB4 is able to efficiently insert Cyt f.

To assess a potential role of ALB4 in the insertion of other components of the cytochrome  $b_6f$  complex, we quantified the amounts of cytochrome  $b_6$  (Cyt  $b_6$ , PetB) and the Rieske protein (PetC) in the *alb4* mutant relative to wild type by immunoblotting (Figure 4, E and F). To enable better quantification, this analysis was conducted using a dilution series of each sample, and so Cyt f was analysed again to provide further corroboration of its reduced abundance in the *alb4* mutant. The data revealed that the Rieske protein is reduced in *alb4* mutants to a similar extent as Cyt f, whereas Cyt  $b_6$  was not significantly reduced. It should

be noted that Cyt f and Cyt b<sub>6</sub> are both encoded by the chloroplast genome, but only one of them is depleted. Therefore, a secondary effect because of reduced chloroplast translation seems unlikely. The two depleted components (Cyt f and the nucleus-encoded Rieske protein) both have only one transmembrane domain, and so the insertion mechanism employed (possibly involving ALB4) might be different from that used by Cyt b<sub>6</sub> with four transmembrane spans. As two components of the cytochrome b<sub>6</sub>f complex are significantly reduced in the *alb4* mutant, we reasoned that photosynthetic capacity might also be reduced in this mutant. To test this, we measured the maximum photochemical efficiency of photosystem II (the  $F_v/F_m$  ratio) in wild type and *alb4* mutants using a chlorophyll fluorescence imaging system. Indeed, there was a small but significant reduction in  $F_v/F_m$  in the *alb4* mutant plants compared to wild type (Student's two-sample t-test based on equal variances,  $p < 0.05$ ) (Supplementary Figure S4).

Overall, it can be concluded that ALB4, together with ALB3, is involved in the insertion of some cytochrome b<sub>6</sub>f subunits. This suggests close functional and potentially physical interactions between ALB3 and ALB4. However, a physical interaction between ALB3 and ALB4 was not detected in a previous study (Benz et al., 2009). To clarify this discrepancy, we examined whether ALB3 and ALB4 can interact *in vivo*.

#### **ALB3 and ALB4 can interact physically *in vivo***

Given that the above analysis revealed significant functional overlap between ALB3 and ALB4, it seemed conceivable that the two proteins interact physically with each other or with the same partners *in vivo*. To address this possibility, we employed immunoprecipitation from isolated chloroplasts following solubilisation using the non-ionic detergent *n*-dodecyl- $\beta$ -D-maltopyranoside (DDM). An interaction between ALB3 and ALB4 could not be found in uncrosslinked chloroplasts, neither in a previous study (Benz et al., 2009) nor in the present study (data not shown). However, by using chloroplasts from transgenic plants expressing FLAG-tagged ALB4, a weak interaction of ALB3 with ALB4-FLAG could be detected after crosslinking with 0.5 mM dithiobis(succinimidyl propionate) (DSP) (Figure 5A); note that ALB3 and ALB4 migrate at significantly different positions during electrophoresis and so were easily distinguished in this analysis (Supplementary Figure S3). Several control proteins, all of which are thylakoid membrane-associated proteins, did not interact with ALB4-FLAG, indicating that the detected ALB3-ALB4 interaction is specific. That the



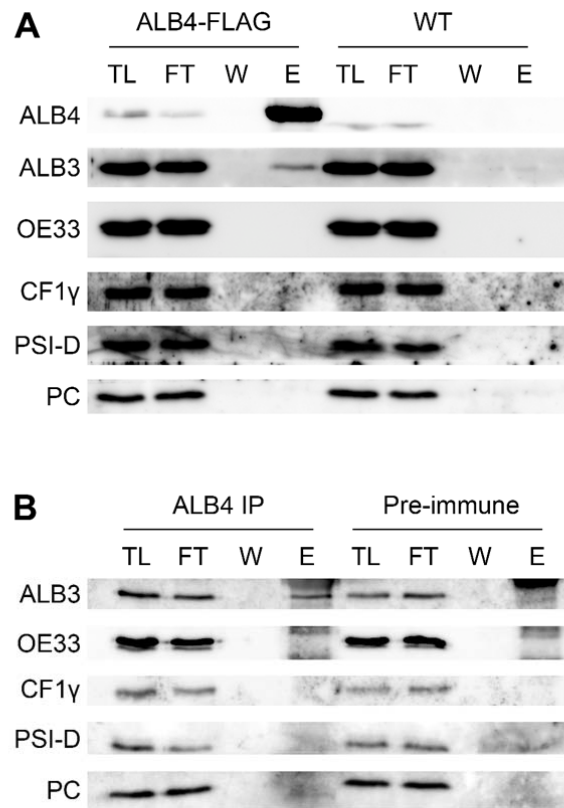


**Figure 5.** Physical interaction between ALB3 and ALB4 *in vivo*.

(A) Immunoprecipitation with anti-FLAG M2 affinity gel using 100 million chloroplasts isolated from plants stably overexpressing an ALB4-FLAG fusion under the CaMV 35S promoter. The chloroplasts were crosslinked with 0.5 mM DSP. TL, total chloroplast lysate (0.45%); FT, flow-through (0.45%); W, final (6<sup>th</sup>) wash (~4.5%); E, eluate (36%). ALB4 was detected with anti-ALB4 antibody; the size shift of ALB4 in the ALB4-FLAG sample compared to wild type corresponds to the size of the FLAG tag. (B) Immunoprecipitation (IP) with anti-ALB4 antibody (or with corresponding pre-immune serum) using 100 million chloroplasts isolated from wild-type plants. Chloroplasts were crosslinked with 0.5 mM DSP. TL, total chloroplast lysate (0.45%); FT, flow-through (0.45%); W, final wash (~4.5%); E, eluate (36%).

ALB3-ALB4 interaction could only be detected following stabilisation using a chemical crosslinker suggests that the ALB3-ALB4 interaction is not stable, but rather is transient in nature or possibly mediated by other factors that bridge the interaction *in vivo*.

Because the ALB4-FLAG lines contain an overexpressed and tagged form of ALB4, one could argue that the observed interaction is an artefact caused by the artificial nature of the experimental system. To exclude this possibility, further immunoprecipitation experiments were performed using an anti-ALB4 antibody and wild-type chloroplasts (Figure 5B). In the immunoprecipitation with anti-ALB4 a weak but specific interaction between ALB3 and ALB4 could be observed, confirming the finding described above. It is particularly interesting that the ATP synthase subunit CF<sub>1</sub> $\gamma$  could not be crosslinked to either native ALB4 (Figure 5B) or overexpressed ALB4-FLAG (Figure 5A), even though it was

shown previously that ALB4 co-migrates with CF<sub>1</sub>γ in two-dimensional blue native/SDS-PAGE experiments (Benz et al., 2009). This finding argues against a non-specific interaction caused by over-crosslinking of the proteins, and therefore supports the relevance of the ALB3-ALB4 interaction detected in this study.

To corroborate the immunoprecipitation data, we performed bimolecular fluorescence complementation (BiFC) experiments using constructs that express ALB3-cYFP, ALB3-nYFP, ALB4-cYFP and ALB4-nYFP under the 35S promoter (nYFP and cYFP are complementary N- and C-terminal fragments of YFP). The data clearly showed that ALB3 and ALB4 can interact *in vivo*. Both combinations of co-transfections (i.e., ALB4-nYFP with ALB3-cYFP and ALB4-cYFP with ALB3-nYFP) produced a signal localized to the thylakoid membranes, in a range of patterns from particulate to filamentous (Figure 6A). Moreover, the previous finding that ALB3 can form dimers at the thylakoid membrane (Dünschede et al., 2011) was confirmed by our analysis, and extended to include the ALB4 homologue (Figure 6A), further emphasizing their functional similarity. The frequency of the transformed, fluorescent protoplasts compared to untransformed, non-fluorescent protoplasts was comparable for ALB3 and ALB4 homodimers and the respective full-length YFP constructs (Figure 6B), and for ALB3-ALB4 heterodimers compared to the ALB4-YFP full-length construct (Figure 6C), suggesting that all interactions are equally efficient *in vivo* (note that the frequencies of positive protoplasts seen for ALB3-YFP and ALB4-YFP were very similar; data not shown). The specificity of the observed interactions was confirmed by the analysis of the ALB fusions in conjunction with fusions to two different control proteins (Supplementary Figure S5).

### **ALB4 can (indirectly) associate with chloroplast SRP components *in vivo***

Since ALB4 could be crosslinked specifically to ALB3, the question arises as to whether it could also be crosslinked to the cpSRP components and cpFtsY (which are well known to act in the same pathway as ALB3). Because anti-FLAG and anti-ALB4 immunoprecipitations gave comparable results for the interactions of ALB3 and ALB4 (Figure 5), further interaction studies were performed by anti-FLAG immunoprecipitation using solubilised ALB4-FLAG chloroplasts. In this way, an interaction between ALB4 and both cpSRP components but not cpFtsY could be observed (Figure 7), supporting the notion that ALB4, like ALB3, acts in the cpSRP pathway. The detected interactions were specific, since ALB4-

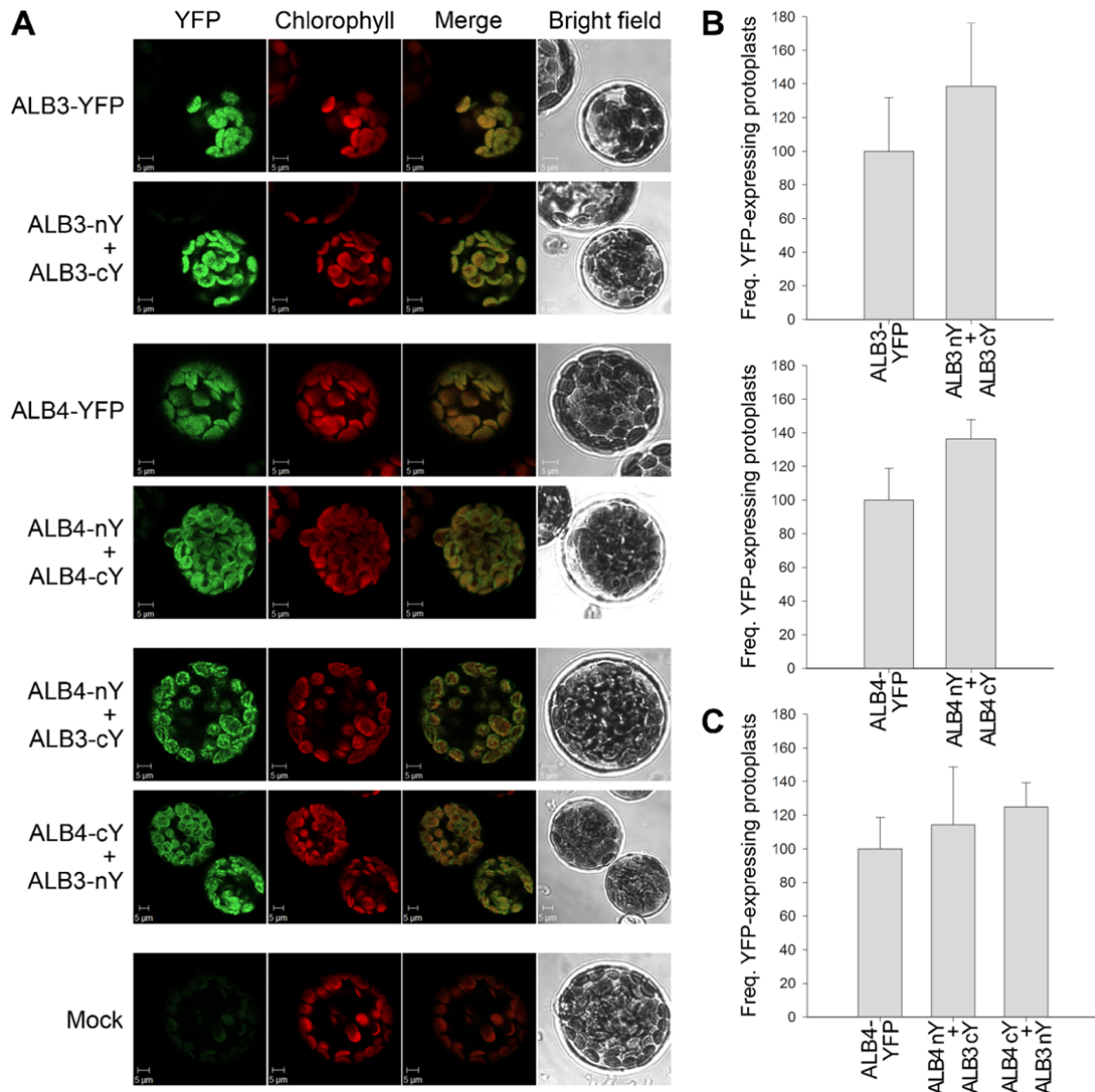


**Figure 6.** Bimolecular fluorescence complementation analysis of ALB3 and ALB4 interactions. (A) Wild-type protoplasts were (co)transfected with the indicated constructs and analysed by confocal microscopy for YFP fluorescence and chlorophyll autofluorescence, and by bright field illumination; “YFP” denotes fusions to full-length YFP, whereas “nY” and “cY” denote fusions to complementary N- and C-terminal fragments of YFP. The formation of ALB3 or ALB4 homodimers, and the interaction between ALB3 and ALB4 in heterodimers, is shown by the reconstitution of the YFP protein leading to fluorescence, as shown by the typical images in the respective panels. No YFP signal was detected in untransformed control protoplasts (Mock). (B) The frequency of protoplasts that displayed YFP reconstitution via ALB3 or ALB4 homodimerization. Values for formation of the homodimers are normalized relative to the frequency observed for the respective full-length YFP construct. (C) The frequency of protoplasts that displayed YFP reconstitution via ALB3-ALB4 heterodimerization (in both directions). Values for formation of heterodimers are normalized relative to the frequency observed for the full-length ALB4-YFP construct. In B and C, all error bars denote standard deviations (n=3).

FLAG could not be crosslinked to abundant components of the photosynthetic apparatus, including LHCP, oxygen evolving complex 33 kDa subunit, and plastocyanin, which were used as negative controls in this experiment.

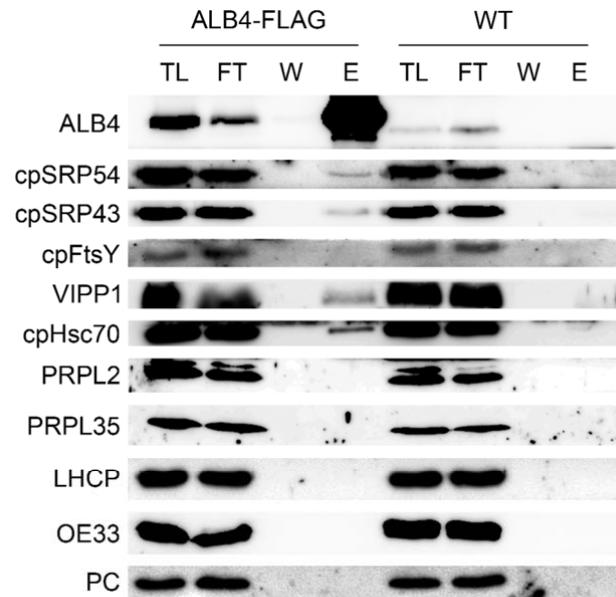


**Figure 7.** Physical interaction of ALB4 with chloroplast SRP components *in vivo*.

Immunoprecipitation with anti-FLAG M2 affinity gel using 100 million chloroplasts isolated from plants stably overexpressing an ALB4-FLAG fusion under the CaMV 35S promoter. Chloroplasts were crosslinked with 0.5 mM DSP. TL, total chloroplast lysate (0.45%); FT, flow-through (0.45%); W, final (6<sup>th</sup>) wash (~4.5%); E, eluate (36%). ALB4-FLAG interacts with the signal recognition particle components cpSRP43 and cpSRP54, as well as with VIPP1 and cpHsc70. However, no interaction between ALB4-FLAG and the plastid ribosomal proteins PRPL2 and PRPL35 (large subunit) could be observed. The abundant photosynthesis-related proteins light harvesting complex protein (LHCP), photosystem I subunit D (PSI-D), oxygen evolving complex 33 kDa subunit (OE33), and plastocyanin (PC) were used as negative controls.

A previous study reported an interaction between *Chlamydomonas* Alb3.2 and vesicle-inducing protein of plastids 1 (VIPP1) (Göhre et al., 2006), which is involved in thylakoid formation and maintenance (Kroll et al., 2001). In Alb3.2 RNAi mutants, both VIPP1 and chloroplast Hsp70 are overproduced, and it was suggested that the VIPP1/cpHsp70 system is involved in the targeting of Alb3.2 in *Chlamydomonas* (Göhre et al., 2006). Therefore, we assessed for possible interactions of ALB4 with VIPP1 and chloroplast Hsp70 cognate (cpHsc70) in *Arabidopsis*. Indeed, clear interactions of ALB4-FLAG with VIPP1 and cpHsc70 could be observed after crosslinking (Figure 7). This implies functional similarity between ALB4 and ancestral Alb3-type proteins. The VIPP1/cpHsp70 system might be involved in the targeting of *Arabidopsis* ALB proteins, or alternatively it might act concomitantly with ALB4 to maintain thylakoid stability and complex assembly, as suggested for *Chlamydomonas* (Göhre et al., 2006).

Because it has been reported before that Oxa1, a mitochondrial homologue of ALB3 and ALB4, can interact with components of the large ribosomal subunit in mitochondria (Jia et al., 2003; Szyrach et al., 2003), and because it was speculated that two conserved motifs in

the ALB3 and ALB4 C-termini could be responsible for ribosome binding (Falk et al., 2010), the interaction of ALB4-FLAG with two plastid ribosomal large-subunit proteins (PRPLs) was also investigated. However, neither PRPL2 nor PRPL35 could be cross-linked to ALB4-FLAG, arguing against a role for ALB4 similar to that of Oxa1 (Figure 7).

### **Phylogenetic analysis of ALB3 and ALB4 supports functional divergence**

Both ALB3 and ALB4 are multi-spanning transmembrane proteins with a substantial C-terminal domain (starting after the fifth transmembrane domain) exposed to the stroma. It has been proposed that differences in their functions are caused by differences in their C-termini, resulting in differing interactions with partner proteins. By the alignment of sequences from several species including *Arabidopsis*, a previous analysis identified four motifs (denoted I, II, III and IV) in the C-terminal domain of ALB3 (Falk et al., 2010). Motifs II and IV were shown to be essential for the binding of ALB3 to cpSRP43, and found to be absent from ALB4; motifs I and III were present in both ALB proteins and dispensable for the cpSRP43 interaction (Falk et al., 2010). These results are not entirely consistent with our observations that ALB4 associates with cpSRP components *in vivo* and shares functional redundancy with ALB3. To begin to address the discrepancy, we first conducted a reassessment for the presence of the motifs using a computer program called meme (Bailey and Elkan, 1994). In accordance with the previous analysis, all four motifs were identified in ALB3, whereas only motifs I and III were clearly present in ALB4 (Figure 8). Our analysis also identified an ALB4-specific motif running from the C-terminal end of motif I and across the position occupied by motif II in ALB3. This indicates that motifs I and II may be part of one larger motif, with its C-terminal end (identified as motif II) being responsible for substrate binding. We also identified an additional conserved region in ALB3 that overlaps with the C-terminal end of motif II, and is very similar to a corresponding region in ALB4 (at least in the Brassicaceae, *A. thaliana* and *B. rapa*) (Figure 8).



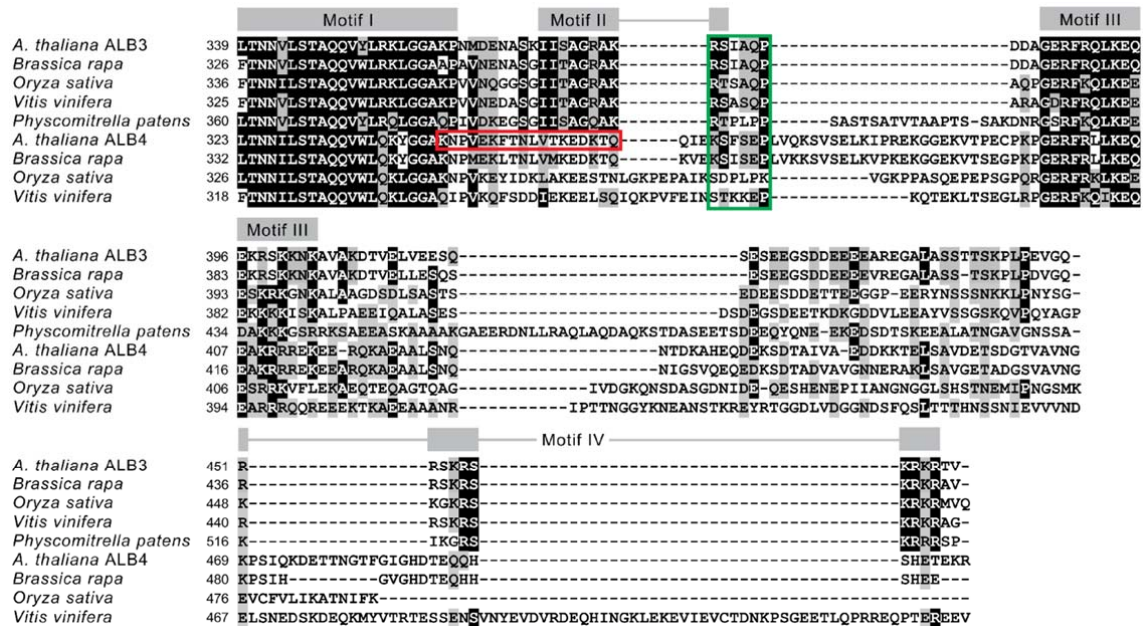


**Figure 8.** Motifs identified in the C-terminal domains of ALB3 and ALB4.

A multiple sequence alignment of the C-terminal regions of ALB3 and ALB4 homologues from different species is shown. The first residue is position 339 in *A. thaliana* ALB3 (and the corresponding position in all other sequences), and represents the start of motif I as defined by Falk et al. (2010). Positions of the motifs are indicated above the alignment. The red box indicates an ALB4-specific motif spanning the positions of motifs I and II, which was identified by the program meme. The green box indicates the position of the extended C-terminal part of motif II, which is present in both ALB3 and ALB4, and is hypothesised to be part of the substrate binding motif. Highly conserved sites are identified by a black background, and similar amino acids by a grey background.

Thus, we hypothesise that the interaction between ALB4 and cpSRP43 observed in our study (Figure 7) is either indirect (e.g., mediated by a mutual partner protein), or occurs via the aforementioned extended motif II that is present in both ALB3 and ALB4. Interestingly, our analysis also showed that all four motifs are present in the ALB3 homologue of the moss *Physcomitrella patens*, implying that the ancestor of all land plants contained an Alb3-type protein with all four motifs, and that two of them were subsequently lost, or highly modified, in ALB4 (Figure 8).

To further assess whether the common ancestor of the ALB proteins was more similar to ALB3 or ALB4, and whether the subsequent evolutionary divergence was greater in the C-termini relative to other parts of the protein, a phylogenetic analysis was conducted. In this work, we analysed the full-length sequences, as well as the N-terminal and C-terminal domains independently. The results indicated that the different parts of the proteins have indeed evolved at different rates. Analysis of the full-length sequences showed that the evolutionary rate in the ALB4 clade has been greater than that in ALB3, as indicated by the differences in branch length between the ALB3 and ALB4 clades (Figure 9A; see

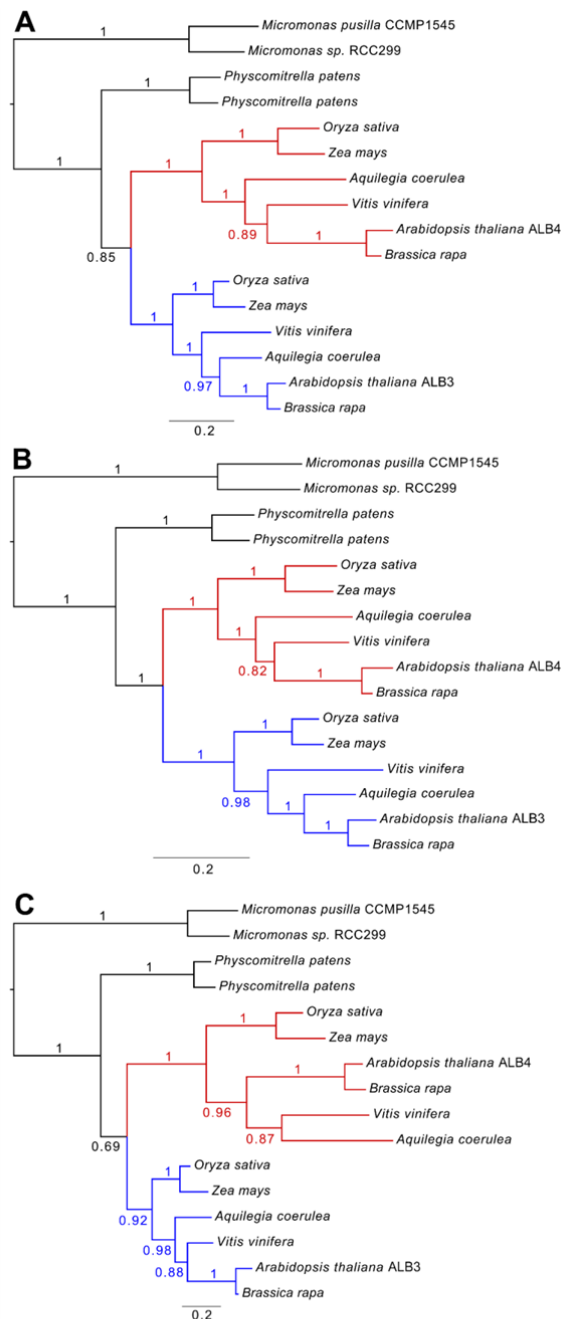


**Figure 9.** Phylogenetic analysis of ALB sequences from different species.

The full-length sequences of ALB3 and ALB4 proteins, as well as their N-terminal and C-terminal domains, were analysed independently. Comparison of the branch lengths indicates that the evolutionary rates have varied in different parts of the proteins. (A) Analysis of full-length sequences shows that the overall rate has been greater in the ALB4 clade (red) than in the ALB3 clade (blue). (B) The N-terminal domain has evolved at an equal rate in the two main clades. (C) An accelerated evolutionary rate occurred in relation to the C-terminal part of the ALB4 proteins. The scale bar below each tree indicates the number of expected changes per site along the branches, and posterior probability values are indicated at each branch.

Supplementary Figure S6 for a more extensive analysis). This is consistent with the notion that ALB4 has undergone greater functional divergence from the ancestral protein. Interestingly, while the N-terminal parts evolved at an equal rate in the two clades (Figure 9B), accelerated evolutionary rates occurred in the C-termini of the ALB4 proteins (Figure

409 9C), thus explaining the overall difference seen with the full-length sequences. These results  
410 are consistent with the aforementioned motif analyses, and support the notion that ALB4  
411 functions have diverged, at least to some extent, from those of ALB3 due to changes in the C-  
412 terminal domain.

413





## Discussion

In this study, we showed that *Arabidopsis alb3 alb4* double mutants have a lower chlorophyll and carotenoid content than *alb3* single mutants, and that the chloroplast ultrastructure of the double mutant is further deteriorated. Therefore, one role of ALB4 in the *alb3* mutant background is likely to be the insertion of some pigment-bearing proteins into the thylakoid membrane, which was not predicted in earlier models of ALB4 function (Benz et al., 2009). Indeed, we could show that Cyt f accumulates in *alb3* mutants but is almost completely absent in *alb3 alb4* double mutants. Moreover, both Cyt f and the Rieske protein are significantly reduced in *alb4* single mutants, even though these mutants have no obvious visible defects. Since it is known that the cytochrome  $b_6f$  complex binds chlorophyll *a* and  $\beta$ -carotene molecules, (Dashdorj et al., 2005; Baniulis et al., 2011), differences in the accumulation of cytochrome complex components between the *alb3* single mutant and the *alb3 alb4* double mutant could be (partly) responsible for the pigmentation differences. The data suggest that ALB4 is involved in the insertion of Cyt f and the Rieske protein, and thus possibly in the biogenesis of the cytochrome  $b_6f$  complex. This notion is supported by the observation that photosynthetic performance (as indicated by the  $F_v/F_m$  ratio) is slightly but significantly reduced in *alb4* mutants compared to wild type. That Cyt f is still present in the *alb4* single mutant but not in the *alb3 alb4* double mutant suggests that both ALB3 and ALB4 may act together in the biogenesis of the cytochrome  $b_6f$  complex.

In a previous study, ALB3 and ALB4 could not be co-immunoprecipitated from isolated thylakoid membranes in the absence of a crosslinker (Benz et al., 2009). Likewise, an interaction between ALB3 and ALB4 could not be detected in the present study using uncrosslinked isolated chloroplasts. This suggests that any interaction between these components may be transient, indirect or lost during protein preparation. Nonetheless, by using crosslinked chloroplasts a specific interaction between ALB3 and ALB4 could be detected. The function of this interaction is unlikely to be reciprocal membrane insertion (i.e., a client-insertase relationship), as ALB4 is still prominently detected in albino *alb3* mutants (Figure 1D) and ALB3 is also detected in *alb4* mutants (Supplementary Figure S3). Our BiFC study not only verified the interaction between ALB3 and ALB4 *in vivo*, but also suggested that this heterodimerization is as frequent as homodimerization. In *Chlamydomonas reinhardtii*, the two paralogous Alb3 proteins, Alb3.1 and Alb3.2, were found to interact with each other and with reaction centre polypeptides, suggesting that both

447 play a role in the assembly of reaction centres (Göhre et al., 2006). This shows that the  
448 interaction between different ALB isoforms for the concerted insertion of a subset of  
449 substrate proteins might not be uncommon.

450 The weak phenotype of *alb4* single mutants suggests that most thylakoid proteins can  
451 be targeted by ALB3 alone. However, as ALB4 is able to interact with ALB3 *in vivo*, it may  
452 form heterodimers which potentially enable optimized insertion of a subset of thylakoid  
453 proteins, relative to ALB3 homodimers, which might be inefficient in these cases. The  
454 discovery that both ALB3 and ALB4 are required for efficient insertion of Cyt f suggests that  
455 this may be one such substrate protein. It is tempting to speculate that ALB4 evolved to  
456 optimize the insertion of specific substrates: that ALB3 alone may insert LHCPs efficiently  
457 and other substrates less efficiently, and that ALB4 increases efficiency when acting together  
458 with ALB3 on the latter substrates. It should be noted that a previous study associated the  
459 release of soluble Cyt f with less stacked thylakoid membranes and a more swollen thylakoid  
460 lumen in *Chlorella saccharophila* chloroplasts (Zuppini et al., 2009). Interestingly, a very  
461 similar phenotype has been described for *Arabidopsis* chloroplasts of *alb4* mutants (Benz et  
462 al., 2009), again supporting the role of ALB4 in the insertion of Cyt f.

463 As it is well known that proteins from the YidC/Oxa1/Alb3 family can function in both  
464 post- and co-translational modes of membrane protein insertion, a role for ALB3 in co-  
465 translational membrane protein insertion that might involve SecY-related SCY1 and  
466 cpSRP54 has been suggested (Zhang and Aro, 2002; Moore et al., 2003). In fact, the ALB3  
467 and ALB4 C-termini both contain two conserved motifs, I and III, which have been suggested  
468 to be involved in SCY1 binding (Falk et al., 2010). Therefore, the question arises as to  
469 whether ALB3 and ALB4 are involved in co-translational protein targeting. The C-terminus  
470 of Oxa1, the mitochondrial homologue of ALB3 and ALB4, is known to interact with the  
471 ribosomal large subunit during co-translational protein insertion (albeit independently of SRP  
472 and the Sec translocon, both of which are absent in mitochondria) (Glick and Von Heijne,  
473 1996; Szyrach et al., 2003). However, here we show that ALB4 does not interact with two  
474 plastid ribosomal proteins of the large subunit, PRPL2 and PRPL35. Also, *alb4* mutants are  
475 not specifically affected in chloroplast-encoded proteins as the reduced Cyt f and Rieske  
476 components are of different genetic origins while the chloroplast-encoded Cyt  $b_6$  component  
477 is not reduced. While this does not exclude the possibility that ALB4 transiently interacts  
478 with other ribosomal proteins or translating proteins, it does argue against an active  
479 participation of ALB4 in the early steps of co-translational membrane protein insertion.

It was previously shown *in vitro* that the C-terminus of ALB3 can interact with cpSRP43 based on motifs which are absent in the ALB4 C-terminus, which consequently cannot interact with cpSRP43 (Falk et al., 2010). Surprisingly, in the present study we found that both cpSRP43 and cpSRP54 can be crosslinked to ALB4 *in vivo*, suggesting an interaction involving other ALB4 motifs (such as the motif II extension identified in this study), or an indirect, bridged interaction between ALB4 and cpSRP43. Since ALB4 interacts also with ALB3, it cannot be established if ALB4 interacts with the cpSRP components directly or via ALB3. Nevertheless, our results provide evidence that ALB4 can participate in processes that involve a close physical proximity to the whole ALB3-cpSRP system. The fact that ALB4 can interact with ALB3, cpSRP43 and cpSRP54 is consistent with a function of ALB4 in the protein insertion process of the ALB3-cpSRP system for a subset of thylakoid proteins, as outlined above. In our experiments, cpFtsY was not crosslinked to ALB4, which is in line with the earlier finding that cpFtsY does not form significant interactions with cpSRP components or ALB3 (Tu et al., 2000). Perhaps the GTP-dependent interaction of cpSRP54 with cpFtsY is too transient to be caught with the conditions used here, even following crosslinking. The detection of ALB4 interactions with VIPP1 and cpHsc70 in the present study is in line with previous studies showing interactions between Alb3.2 and VIPP1 (Göhre et al., 2006), and between soluble VIPP1 and cpHsc70 (Liu et al., 2007), in *Chlamydomonas reinhardtii*. Perhaps the VIPP1 system and the ALB3-cpSRP system cooperate in thylakoid biogenesis, coordinating the extension of the lipid layers with protein insertion.

Our phylogenetic analyses showed that the N-terminal parts of the ALB3/4 proteins evolved at similar rates in angiosperms, and that there was a shift in evolutionary rate in relation to the C-terminal domains following a gene duplication in an ancient angiosperm Alb3 protein. The gene duplication would have led to a redundancy of Alb3 genes that enabled one of the copies (the ALB4 progenitor) to mutate and eventually evolve a divergent function, while the other (the ALB3 progenitor) retained the original function performed by the ancestral protein. The accelerated evolutionary rate led to the loss (or extensive modification) of two potential binding motifs (II and IV) in ALB4. Nonetheless, our results show that cpSRP43 can to some extent interact with ALB4 *in vivo*, suggesting an interaction involving motifs other than II and IV (e.g., the extended motif II described here, or others present elsewhere in the C-terminal domain or even in one of the loops), or an indirect, bridged interaction. Motifs I and III, which are present in both ALB3 and ALB4, have been

suggested to be responsible for ribosome binding (Falk et al., 2010). However, we were unable to detect an interaction of ALB4 with two chloroplast ribosome components.

In summary, our results point to a role for ALB4 in inserting some proteins (e.g., Cyt f, and potentially other components of pigment-bearing complexes) into thylakoids in the *alb3* background, while in the wild-type background ALB4 might act together with ALB3 and thus optimize its function for the assembly of the cytochrome  $b_6f$  complex and possibly other complexes. Although ALB3 is certainly crucial for the insertion of LHC components, and ALB4 might influence the stability of non-photosynthetic thylakoid complexes (Benz et al., 2009), a sharp separation of the functions of the two paralogues is not supported by the presented data. Both genetic and physical interaction studies suggest some functional overlap between ALB3 and ALB4, but they may have evolved such that ALB3 plays key roles during membrane protein insertion while ALB4 optimizes this process for a subset of substrates. Thus, ALB3 and ALB4 likely contribute differentially but synergistically to the same process of protein insertion into the thylakoids via the ALB3-cpSRP pathway.

## Materials and Methods

### Plant growth and genotyping

Mutant seeds were ordered from the Nottingham *Arabidopsis* Stock Centre (NASC; *alb3*: GABI\_293B08/N324478; *alb4*: Salk\_136199/N636199). They were grown directly on soil (*alb4*, kanamycin resistance marker silenced), or *in vitro* on half-strength Murashige and Skoog (MS) plates containing 0.5% (w/v) sucrose and 11.25 µg/ml sulfadiazine (for *alb3* selection) after surface sterilisation of the seeds and two days stratification at 4°C as described previously (Aronsson and Jarvis, 2002). After initial germination and growth for 14 days on the standard medium indicated above, albino seedlings (homozygous *alb3* mutants and *alb3 alb4* double mutants) were transferred to half-strength MS plates containing 3% (w/v) sucrose for further growth. Plants were grown in ~100 µmol/m<sup>2</sup>/s white light under long-day cycles (16 h light, 8 h dark) except where short-day conditions (8 h light, 16 h dark) are specifically indicated.

For genotyping, the following primers were used: *alb4* forward, 5'-CCTTGCA-GGTACAGTATGTTA-3'; *alb4* reverse, 5'-CTGTTGCATAGAAGGATTTTCG-3'; *alb3* forward, 5'-CGCTTCGTATTGAGAGATATA-3'; *alb3* reverse, 5'-GAGAGGA-TACAACTAGAGACA-3'. For T-DNA specific PCRs, the *alb4* forward primer was combined with SALK LBb1, 5'-GCGTGGACCGCTTGCTGCAACT-3', and the *alb3* reverse primer was combined with GK-LB, 5'-CCCATTTGGACGTGAATGTAGACAC-3'.

### Total chlorophyll and carotenoid measurements, transmission electron microscopy, and fluorescence measurements

Pigment extraction and measurement was based on a method described previously (Czarnecki et al., 2011). Approximately 50 mg of 3-week-old seedlings were frozen in liquid nitrogen, ground and then covered with 300 µl of 80% acetone containing 10 µM KOH. The samples were vortexed for at least one minute and then centrifuged at 10,000 g for 10 minutes in a microcentrifuge. Absorbances of the supernatant were measured at 663 nm, 647 nm and 470 nm, and the amounts of total chlorophyll per mg fresh weight were calculated as previously described (Czarnecki et al., 2011).

For transmission electron microscopy, the first true leaves from 17-day-old plants were used, and the service of the University of Leicester Electron Microscope Laboratory (Faculty of Medicine and Biological Sciences) was employed. Leaves were excised from the plant and fixed overnight in 4% glutaraldehyde / 2% formaldehyde in 0.1 M sodium cacodylate buffer with 2 mM calcium chloride (pH 7.2), and then washed in the same cacodylate/CaCl<sub>2</sub> buffer. The tissue was then fixed with 1% OsO<sub>4</sub> / 1.5% potassium ferricyanide for 3 hours, washed with distilled, de-ionised water, and finally tertiary fixed with 2% uranyl acetate for 1 hour. The tissue was serially dehydrated through ethanol and propylene oxide and embedded in Spurr's modified low viscosity resin. Thin sections of ~80 nm thickness were cut using a Reichert Ultracut S ultramicrotome, collected onto copper mesh grids, and stained with Reynolds' lead citrate. The grids were viewed under a JEOL JEM-1400 electron microscope at 80 kV. Digital images were recorded using a SIS digital camera and iTEM software (Glauert, 1998; Hyman and Jarvis, 2011).

The  $F_v/F_m$  ratio was measured using a CF Imager chlorophyll fluorescence imaging system (Technologica, Essex, UK). Wild type and *alb4* mutants were grown on half-strength MS medium containing 0.5% (w/v) sucrose as described above. Four plates with 17-day-old seedlings from each genotype were dark-adapted for one hour and subsequently recorded under saturating light pulses of 6000  $\mu\text{mol photons/m}^2/\text{s}$ . The  $F_v/F_m$  ratio values were determined by the CF Imager's software (Baker, 2008; Gorecka et al., 2014) for four quarters of each plate independently, resulting in 16 individual measurements per genotype.

## Antibody production and immunoblotting

The anti-ALB4 antibody was generated by cloning the coding sequence of the C-terminal 155 amino acids of ALB4 (soluble part) into pQE-30 (Qiagen) using BamHI and PstI following amplification using primers ALB4-His-F, 5'-GGGGGATCCCCAGTGGAGAAATTCATA-3', and ALB4-His-R, 5'-GGCCTGCAGGTTACCTCTTCTGTTCAT-3'. Transformed XL1-Blue cells were grown in the presence of 1% glucose in order to repress the lac operon and avoid leaky expression. Expression of His-tagged ALB4 C-terminus was induced with 1 mM isopropyl  $\beta$ -D-1-thiogalactopyranoside (IPTG) and the cells were lysed by sonication in lysis buffer (50 mM NaH<sub>2</sub>PO<sub>4</sub>, 300 mM NaCl, 10 mM imidazole, pH 8.0). The lysate was put onto polypropylene columns containing Ni-NTA resin (Qiagen), washed with wash buffer (50 mM

NaH<sub>2</sub>PO<sub>4</sub>, 300 mM NaCl, 20 mM imidazole, pH 8.0), and the proteins were eluted in elution buffer (50 mM NaH<sub>2</sub>PO<sub>4</sub>, 300 mM NaCl, 250 mM imidazole, pH 8.0). Purified protein was sent to Harlan Serlab (Loughborough, UK) for antibody production in rabbits and the antiserum was affinity purified using the original antigen. The anti-ALB3 antibody was a gift from Prof. D. Schünemann (Gerdes et al., 2006; Asakura et al., 2008). The cpSRP and cpFtsY antibodies were a gift from Prof. M. Nakai. Immunoblots were performed using standard methods with 12% polyacrylamide gels and nitrocellulose membranes (Kovacheva et al., 2005).

### **Bimolecular fluorescence complementation**

For BiFC, the vectors pSAT4(A)-cEYFP-N1 and pSAT4(A)-nEYFP-N1 were used (Lee et al., 2008). For the ALB4 constructs, amplification of the wild-type cDNA employed the primers ALB4-BiFC-F, 5'-AAGAGATCTCAAAGCAAGAACACAACA-3' and ALB4-BiFC-R, 5'-AAGGTCGACTCCTCCTCTCTGTTTCATGAGA-3'; for the ALB3 constructs, the primers were ALB3-BiFC-F, 5'-AAAGAATTCTCTCTATCTTCTTCTTCGTCTCTT-3' and ALB3-BiFC-R, 5'-AAAGTCGACATACAGTGC GTTTCGCTTCGA-3'; for the OEP7 constructs, the primers were OEP7-5 EcoRI, 5'-AAGAATTCATGGGAAAACTTCGGGA-3' and OEP7-3 Sall, 5'-TTGTCGACACAAACCCTCTTTGGATGT-3'; for the PSI-D constructs, the primers were PSI-D XhoI Fwd, 5'-TTCTCGAGATGGCAACTCAAGCCGCC-3' and PSI-D BamHI Rev, 5'-CCGGATCCCCAAATCATAACTTTGTTTG-3'. Purified PCR products and vectors were digested with BglII and Sall (ALB4), EcoRI and Sall (ALB3 and OEP7), or XhoI and BamHI (PSI-D). The digested PCR products were ligated into the linearized vectors.

Protoplasts from 4-5-week-old wild-type plants grown on soil were isolated using the tape-*Arabidopsis*-sandwich method (Wu et al., 2009). Approximately  $1 \times 10^5$  protoplasts and 5 µg of plasmid DNA were used per (co)transfection in 40% (w/v) PEG-4000 solution (Wu et al., 2009). Samples were analysed 16-18 hours after (co)transfection using a Zeiss LSM 510 META laser-scanning confocal microscope using a C-Apochromat 40x/1.2 W corr. objective. To detect YFP, a 514 nm excitation from a 5 mW Argon ion laser with an HFT 458/514 primary dichroic mirror and a 535 to 590 nm emission filter was used. To simultaneously detect chlorophyll autofluorescence, an NFT 635 vis long-pass filter was used. The frequency



of protoplasts that successfully expressed YFP fluorescence was estimated by counting the number of positives in the total number of protoplasts observed per microscope field, in 20-25 microscope fields per (co)transfection. The frequency of YFP-expressing protoplasts in the co-transfections was normalised to the frequency of the respective full-length YFP fusion used as a control. Images were processed with the Zeiss LSM Image Browser software. Each (co)transfection was conducted three times, with the same result, and typical images are shown.

### **Creation of ALB4-FLAG lines**

The ALB4 coding sequence without the stop codon was cloned using Gateway® technology (Invitrogen) into a C-terminal FLAG tag binary vector derived from pEarlyGate 302 (Earley et al., 2006) containing a 35S promoter and spectinomycin and hygromycin resistance markers. *Agrobacterium* GV3101 was transformed by the freeze-thaw method (Holsters et al., 1978) and six-week-old flowering wild-type plants were transformed by the floral dip method (Clough and Bent, 1998). ALB4-FLAG overexpressing T<sub>2</sub> lines were confirmed by immunoblotting using our anti-ALB4 antibody and using an anti-FLAG antibody (Sigma). Finally, an ALB4-FLAG line was selected (line 32) that showed a 1:4 segregation on selective medium, indicating a single T-DNA insertion, and that showed a high transgene transcription rate by RT-PCR.

### **Chloroplast isolation and crosslinking**

Chloroplasts of two-week-old wild-type plants or plants overexpressing the ALB4-FLAG construct were isolated as described previously (Aronsson and Jarvis, 2002). Freshly isolated chloroplasts were counted using a counting chamber (Weber Scientific) and normalised to 100 million chloroplasts in 300 ml HEPES-MgSO<sub>4</sub>-sorbitol (HMS) buffer (Aronsson and Jarvis, 2002). For crosslinking, 0.5 mM DSP (in dimethyl sulfoxide) was added to the chloroplasts prior to incubation on ice for 15 minutes. Reactions were then quenched with 50 mM glycine for 15 minutes before the chloroplasts were pelleted by centrifugation at maximum speed and 4°C for 30 seconds using an Eppendorf Centrifuge 5417 R with an EL 082 rotor. The supernatant was removed and the pellet was used for immunoprecipitations.

## **Immunoprecipitation**

Anti-FLAG-immunoprecipitation was performed with 100 million crosslinked chloroplasts from the ALB4-FLAG expressing line, and with an equal number of wild-type chloroplasts as control. The chloroplasts were solubilised in solubilisation buffer (20 mM Tris-HCl, 150 mM NaCl, 1 mM EDTA, 10% glycerol, 1% *n*-dodecyl- $\beta$ -D-maltopyranoside (DDM), pH 7.5) containing 1 $\times$  protease inhibitor cocktail (cOmplete, Mini, EDTA-free, Roche). Following the manufacturer's guidelines, 60  $\mu$ l of Anti-FLAG M2 Affinity Gel (Sigma) per sample was pre-equilibrated in solubilisation buffer and the ALB4-FLAG (and control) was incubated for 2 hours by rotating at 4°C. The Anti-FLAG M2 Affinity Gel was then washed six times with wash buffer (20 mM Tris-HCl, 150 mM NaCl, 1 mM EDTA, 10% glycerol, 0.3% DDM, pH 7.5) and collecting each time the resin by quick centrifugation, before 50  $\mu$ l of 2 $\times$  SDS-PAGE sample loading buffer was added. Per experiment, 18  $\mu$ l of the denatured eluate was loaded.

Anti-ALB4 immunoprecipitation was performed with 100 million crosslinked chloroplasts from wild-type plants. The chloroplasts were solubilised as described above, and equal volumes of anti-ALB4 antibody and pre-immune serum were added to the lysate of the sample and the control, respectively. Both were incubated for 3 hours by rotating at 4°C. Protein A sepharose CL-4B (GE Healthcare) (50 mg) was pre-equilibrated in 200  $\mu$ l sterile water on ice for 30 minutes, then washed three times with water and once with solubilisation buffer. To the samples, 100  $\mu$ l of this slurry was added, prior to rotation for 2 hours at 4°C and then washing as described above. Again, 50  $\mu$ l of 2 $\times$  SDS-PAGE sample loading buffer was added to the slurry, and 18  $\mu$ l of the denatured eluate was loaded per experiment.

## **Phylogenetic analysis**

Homologous ALB3 and ALB4 amino acid sequences from land plant species were obtained using BLAST 2.2.26+ (Camacho et al., 2009). In addition, green algal sequences were included in the analysis in order to root the tree (Supplementary Table S1). Datasets were downloaded from [www.phytozome.net](http://www.phytozome.net) and the blast searches were run locally. The sequences were aligned using mafft-linsi (Kato and Standley, 2013) and the independently analysed regions of the alignment matrix were obtained by excluding regions (the N-terminus and the C-terminus, respectively) using the alignment editor Seaview (Gouy et al., 2010). Independent analyses on the full length sequences, the N-termini corresponding to residues 0-338 in *Arabidopsis* ALB3 (Falk et al., 2010), and the C-termini (corresponding to residues 339-462, and including all four motifs of *Arabidopsis* ALB3) were performed using MrBayes v.3.2.2 (Ronquist et al., 2012) and the Beagle library (v1.0) for likelihood calculations (Ayres et al., 2012). A mixed model of amino acid substitutions was used for all three analyses and the mcmc chains were run for 1,000,000 generations sampling trees every 1000 generations. An extended set of sequences (see Supplementary Table S1 and Figure S2) was also analysed and the mcmc sampling was then done for 2,000,000 generations. Convergence and mixing of the mcmc chains was analysed using Tracer v.1.5 (Rambaut and Drummond, 2007), after which 50% majority-rule consensus phylograms were produced using the default settings.

### Identification of sequence motifs

The motif search analysis was performed on the meme web server (<http://meme.nbcr.net/meme/>) (Bailey and Elkan, 1994) by searching for a maximum of 20 motifs, allowing each motif to occur zero or one time and to be of width 6-300 residues. The analysis was performed on the two different datasets containing 25 angiosperm ALB3 and ALB4 sequences each, and an out-group dataset of seven sequences from green algae and the moss *Physcomitrella patens*. For further details see: <http://dx.doi.org/10.6084/m9.figshare.1061978>.

### Acknowledgements

We thank Natalie Allcock and Stefan Hyman for electron microscopy, Paula Töpel for graphical support, Ramesh Patel for technical support, Feijie Wu for the OEP7 BiFC constructs, and Qihua Ling for help with the CF Imager chlorophyll fluorescence imaging system. We are grateful to Prof. D. Schünemann and Prof. M. Nakai for kindly providing antibodies, and to Prof. Stanton Gelvin for providing the BiFC vectors. This manuscript is dedicated to the memory of Stefan Hyman who sadly passed away on 26<sup>th</sup> March 2015.

## Figure Legends

**Figure 1.** Basic characteristics and genetic analysis of the *A. thaliana alb4* and *alb3* mutants. (A) Gene diagrams of *A. thaliana ALB4* and *ALB3* with the T-DNA insertions of the *alb4* and *alb3* mutant lines shown. Protein-coding exons are represented by black boxes, untranslated regions by grey boxes, and introns by thin lines between the boxes. T-DNA insertion sites are indicated precisely, but insertion sizes are not to scale. ATG, translation initiation codon; Stop, translation termination codon; p(A), polyadenylation site; LB, T-DNA left border. (B) Wild-type and *alb4* mutant plants (Salk\_136199) were directly grown on soil under short day (8h light/16h dark) or long day (16h light/8h dark) conditions. Pictures were taken after 7 weeks (Short day) and 4 weeks (Long day). (C) Genotype analysis by genomic PCR. Heterozygous *alb3* mutants (GK\_293B08) and *alb3/+ alb4/alb4* plants were visibly indistinguishable from wild type, but both contained the *alb3* T-DNA insertion (I; lanes 1 and 4); *alb3/+ alb4/alb4* plants additionally contained the homozygous *alb4* T-DNA insertion (III; lanes 3 and 6) but not the wild-type *ALB4* allele (II; lanes 2 and 5). The ladder (lane 0, left side) includes standards of the following sizes, starting at the bottom: 0.3, 0.4, 0.5, 0.65, 0.85, 1.0, 1.65 and 2.0 kb. (D) Immunoblot analysis of total protein extracts from 3-week-old albino plants. The *alb3 alb4* double mutant seedlings contained considerably less ALB4 protein than *alb3* single mutants. (E) Segregation analysis of the progeny of three individual *alb3/+ alb4/alb4* (“het/hom”) plants. Values are means of the percentages of green and albino progeny from each of the three parent plants. The error bars denote standard deviations.

**Figure 2.** Phenotypic analysis of *alb3 alb4* double-mutant plants.

(A) Albino seedlings derived from the segregating progeny of *alb3/+* or *alb3/+ alb4/alb4* plants grown *in vitro* on MS medium supplemented with 0.5% sucrose were transferred to MS medium containing 3% sucrose 2 weeks after germination (upper panels) and allowed to grow on for an additional 1 week (lower panels). (B) Chlorophyll *a* (Chl *a*) and chlorophyll *b* (Chl *b*) were measured in µg/mg fresh weight using 3-week-old seedlings grown *in vitro* as described above. The ratio of chlorophyll *a* to chlorophyll *b* (Chl *a*/Chl *b*) is larger than 1 for *alb3* but smaller than 1 for *alb3 alb4*. (C) Total carotenoid (Car) content was measured in

µg/mg fresh weight using similarly grown 3-week-old seedlings. All error bars denote standard errors (n=3).

**Figure 3.** Transmission electron micrographs of *alb3* single and *alb3 alb4* double mutants. (A) Transmission electron micrograph images of mesophyll cell plastids from the first true leaves of 17-day-old seedlings grown *in vitro*. All images show plastids at the same scale; the black scale bar in the wild type image corresponds to 2 µm. The left image of *alb3* shows a starch grain in the middle of the plastid. The *alb3* plastids generally contain a few thylakoid membranes, while these are lacking almost completely in the *alb3 alb4* double mutants. In the *alb3 alb4* double mutants, large round plastids with many vesicles occur roughly at the same frequency as relatively flat plastids without vesicles. (B) Average number of thylakoids, vesicles and starch grains found in plastids from *alb3* single and *alb3 alb4* double mutants. Numbers in brackets denote total numbers of plastids used for counting. The plastid images analysed were derived from three biological replicates. Error bars denote standard errors (n shown in brackets).

**Figure 4.** Accumulation of thylakoid proteins in *alb3*, *alb4* and double-mutant plants. (A) Western blot analysis of total protein extracts from 3-week-old seedlings. All seedlings were grown on MS medium containing 0.5% sucrose. The *alb3* and *alb3 alb4* seedlings were transferred to medium containing 3% sucrose at 2 weeks post germination. Sample loading was normalized according to the intensity of the cpHsc70 band. (B) Western blot analysis of total protein extracts from 2-week-old seedlings grown on MS medium containing 0.5% sucrose. (C) Band intensity quantification of the data shown in panel A, normalized according to the cpHsc70 data. Error bars denote standard deviations (n=3). The average Cyt f value for wild type has been set to 1. (D) Band intensity quantification of the data shown in panel B, prepared exactly as described for panel C. (E) Western blot analysis of total protein extracts from 2-week-old seedlings grown on MS medium containing 0.5% sucrose. A series of 10, 20 and 40 µg of total protein was loaded for each genotype, as indicated. For Cyt f and the Rieske protein, two different exposures are shown (strong and weak), to better illustrate the differences in signal intensity. (F) Band intensity quantification of the data shown in panel E, prepared exactly as described for panel C.

778

779

780 **Figure 5.** Physical interaction between ALB3 and ALB4 *in vivo*.

781 (A) Immunoprecipitation with anti-FLAG M2 affinity gel using 100 million chloroplasts  
782 isolated from plants stably overexpressing an ALB4-FLAG fusion under the CaMV 35S  
783 promoter. The chloroplasts were crosslinked with 0.5 mM DSP. TL, total chloroplast lysate  
784 (0.45%); FT, flow-through (0.45%); W, final (6<sup>th</sup>) wash (~4.5%); E, eluate (36%). ALB4 was  
785 detected with anti-ALB4 antibody; the size shift of ALB4 in the ALB4-FLAG sample  
786 compared to wild type corresponds to the size of the FLAG tag. (B) Immunoprecipitation (IP)  
787 with anti-ALB4 antibody (or with corresponding pre-immune serum) using 100 million  
788 chloroplasts isolated from wild-type plants. Chloroplasts were crosslinked with 0.5 mM DSP.  
789 TL, total chloroplast lysate (0.45%); FT, flow-through (0.45%); W, final wash (~4.5%); E,  
790 eluate (36%).

791

792 **Figure 6.** Bimolecular fluorescence complementation analysis of ALB3 and ALB4  
793 interactions.

794 (A) Wild-type protoplasts were (co)transfected with the indicated constructs and analysed by  
795 confocal microscopy for YFP fluorescence and chlorophyll autofluorescence, and by bright  
796 field illumination; “YFP” denotes fusions to full-length YFP, whereas “nY” and “cY” denote  
797 fusions to complementary N- and C-terminal fragments of YFP. The formation of ALB3 or  
798 ALB4 homodimers, and the interaction between ALB3 and ALB4 in heterodimers, is shown  
799 by the reconstitution of the YFP protein leading to fluorescence, as shown by the typical  
800 images in the respective panels. No YFP signal was detected in untransformed control  
801 protoplasts (Mock). (B) The frequency of protoplasts that displayed YFP reconstitution via  
802 ALB3 or ALB4 homodimerization. Values for formation of the homodimers are normalized  
803 relative to the frequency observed for the respective full-length YFP construct. (C) The  
804 frequency of protoplasts that displayed YFP reconstitution via ALB3-ALB4  
805 heterodimerization (in both directions). Values for formation of heterodimers are normalized  
806 relative to the frequency observed for the full-length ALB4-YFP construct. In B and C, all  
807 error bars denote standard deviations (n=3).

808

**Figure 7.** Physical interaction of ALB4 with chloroplast SRP components *in vivo*.

Immunoprecipitation with anti-FLAG M2 affinity gel using 100 million chloroplasts isolated from plants stably overexpressing an ALB4-FLAG fusion under the CaMV 35S promoter. Chloroplasts were crosslinked with 0.5 mM DSP. TL, total chloroplast lysate (0.45%); FT, flow-through (0.45%); W, final (6<sup>th</sup>) wash (~4.5%); E, eluate (36%). ALB4-FLAG interacts with the signal recognition particle components cpSRP43 and cpSRP54, as well as with VIPP1 and cpHsc70. However, no interaction between ALB4-FLAG and the plastid ribosomal proteins PRPL2 and PRPL35 (large subunit) could be observed. The abundant photosynthesis-related proteins light harvesting complex protein (LHCP), photosystem I subunit D (PSI-D), oxygen evolving complex 33 kDa subunit (OE33), and plastocyanin (PC) were used as negative controls.

**Figure 8.** Motifs identified in the C-terminal domains of ALB3 and ALB4.

A multiple sequence alignment of the C-terminal regions of ALB3 and ALB4 homologues from different species is shown. The first residue is position 339 in *A. thaliana* ALB3 (and the corresponding position in all other sequences), and represents the start of motif I as defined by Falk et al. (2010). Positions of the motifs are indicated above the alignment. The red box indicates an ALB4-specific motif spanning the positions of motifs I and II, which was identified by the program meme. The green box indicates the position of the extended C-terminal part of motif II, which is present in both ALB3 and ALB4, and is hypothesised to be part of the substrate binding motif. Highly conserved sites are identified by a black background, and similar amino acids by a grey background.

**Figure 9.** Phylogenetic analysis of ALB sequences from different species.

The full-length sequences of ALB3 and ALB4 proteins, as well as their N-terminal and C-terminal domains, were analysed independently. Comparison of the branch lengths indicates that the evolutionary rates have varied in different parts of the proteins. (A) Analysis of full-length sequences shows that the overall rate has been greater in the ALB4 clade (red) than in the ALB3 clade (blue). (B) The N-terminal domain has evolved at an equal rate in the two main clades. (C) An accelerated evolutionary rate occurred in relation to the C-terminal part of the ALB4 proteins. The scale bar below each tree indicates the number of expected



840 changes per site along the branches, and posterior probability values are indicated at each  
841 branch.

## Parsed Citations

**Aronsson H, Jarvis P (2002) A Simple Method for Isolating Import-competent Arabidopsis Chloroplasts. FEBS Lett. 529: 215-220**

Pubmed: [Author and Title](#)

CrossRef: [Author and Title](#)

Google Scholar: [Author Only](#) [Title Only](#) [Author and Title](#)

**Asakura Y, Kikuchi S, Nakai M (2008) Non-identical Contributions of two Membrane-bound cpSRP Components, cpFtsY and Alb3, to Thylakoid Biogenesis. Plant J. 56: 1007-1017**

Pubmed: [Author and Title](#)

CrossRef: [Author and Title](#)

Google Scholar: [Author Only](#) [Title Only](#) [Author and Title](#)

**Ayres DL, Darling A, Zwickl DJ, Beerli P, Holder MT, Lewis PO, Huelsenbeck JP, Ronquist F, Swofford DL, Cummings MP, Rambaut A, Suchard MA (2012) BEAGLE: An Application Programming Interface and High-performance Computing Library for Statistical Phylogenetics. Syst. Biol. 61: 170-173**

Pubmed: [Author and Title](#)

CrossRef: [Author and Title](#)

Google Scholar: [Author Only](#) [Title Only](#) [Author and Title](#)

**Bailey TL, Elkan C (1994) Fitting a Mixture Model by Expectation Maximization to Discover Motifs in Biopolymers. Proc. Int. Conf. Intell. Syst. Mol. Biol. 2: 28-36**

Pubmed: [Author and Title](#)

CrossRef: [Author and Title](#)

Google Scholar: [Author Only](#) [Title Only](#) [Author and Title](#)

**Baker NR (2008) Chlorophyll fluorescence: a probe of photosynthesis in vivo. Annu. Rev. Plant Biol. 59: 189-113**

Pubmed: [Author and Title](#)

CrossRef: [Author and Title](#)

Google Scholar: [Author Only](#) [Title Only](#) [Author and Title](#)

**Baniulis D, Zhang H, Zakharova T, Hasan SS, Cramer WA (2011) Purification and Crystallization of the Cyanobacterial Cytochrome b6f Complex. Methods Mol. Biol. 684: 65-77**

Pubmed: [Author and Title](#)

CrossRef: [Author and Title](#)

Google Scholar: [Author Only](#) [Title Only](#) [Author and Title](#)

**Bellafiore S, Ferris P, Naver H, Gohre V, Rochaix JD (2002) Loss of Albino3 Leads to the Specific Depletion of the Light-harvesting System. Plant Cell 14: 2303-2314**

Pubmed: [Author and Title](#)

CrossRef: [Author and Title](#)

Google Scholar: [Author Only](#) [Title Only](#) [Author and Title](#)

**Benz M, Bals T, Gugel IL, Piotrowski M, Kuhn A, Schunemann D, Soll J, Ankele E (2009) Alb4 of Arabidopsis Promotes Assembly and Stabilization of a Non Chlorophyll-binding Photosynthetic Complex, the CF1CF0-ATP Synthase. Mol. Plant 2: 1410-1424**

Pubmed: [Author and Title](#)

CrossRef: [Author and Title](#)

Google Scholar: [Author Only](#) [Title Only](#) [Author and Title](#)

**Camacho C, Coulouris G, Avagyan V, Ma N, Papadopoulos J, Bealer K, Madden TL (2009) BLAST+: Architecture and Applications. BMC Bioinformatics 10: 421**

Pubmed: [Author and Title](#)

CrossRef: [Author and Title](#)

Google Scholar: [Author Only](#) [Title Only](#) [Author and Title](#)

**Clough SJ, Bent AF (1998) Floral Dip: A Simplified Method for Agrobacterium-mediated Transformation of Arabidopsis thaliana. Plant J. 16: 735-743**

Pubmed: [Author and Title](#)

CrossRef: [Author and Title](#)

Google Scholar: [Author Only](#) [Title Only](#) [Author and Title](#)

**Constan D, Patel R, Keegstra K, Jarvis P (2004) An Outer Envelope Membrane Component of the Plastid Protein Import Apparatus Plays an Essential Role in Arabidopsis. Plant J. 38: 93-106**

Pubmed: [Author and Title](#)

CrossRef: [Author and Title](#)

Google Scholar: [Author Only](#) [Title Only](#) [Author and Title](#)

**Czarnecki O, Peter E, Grimm B (2011) Methods for Analysis of Photosynthetic Pigments and Steady-state Levels of Intermediates of Tetrapyrrole Biosynthesis. Methods Mol. Biol. 775: 357-385**

Pubmed: [Author and Title](#)

CrossRef: [Author and Title](#)

Google Scholar: [Author Only](#) [Title Only](#) [Author and Title](#)

**Dalbey RE, Kuhn A, Zhu L, Kiefer D (2014) The Membrane Insertase YidC. Biochim. Biophys. Acta 1843: 1489-1496**

Pubmed: [Author and Title](#)

CrossRef: [Author and Title](#)

Google Scholar: [Author Only](#) [Title Only](#) [Author and Title](#)

**Dashdorj N, Zhang H, Kim H, Yan J, Cramer WA, Savikhin S (2005) The single chlorophyll a molecule in the cytochrome b6f complex: unusual optical properties protect the complex against singlet oxygen. Biophys. J. 88: 4178-4187**

Pubmed: [Author and Title](#)  
CrossRef: [Author and Title](#)  
Google Scholar: [Author Only](#) [Title Only](#) [Author and Title](#)

**Dünschede B, Bals T, Funke S, Schünemann D (2011) Interaction Studies between the Chloroplast Signal Recognition Particle Subunit cpSRP43 and the Full-length Translocase Alb3 Reveal a Membrane-embedded Binding Region in Alb3 Protein. J. Biol. Chem. 286: 35187-35195**

Pubmed: [Author and Title](#)  
CrossRef: [Author and Title](#)  
Google Scholar: [Author Only](#) [Title Only](#) [Author and Title](#)

**Earley KW, Haag JR, Pontes O, Oppen K, Juehne T, Song K, Pikaard CS (2006) Gateway-compatible Vectors for Plant Functional Genomics and Proteomics. Plant J. 45: 616-629**

Pubmed: [Author and Title](#)  
CrossRef: [Author and Title](#)  
Google Scholar: [Author Only](#) [Title Only](#) [Author and Title](#)

**Falk S, Ravaut S, Koch J, Sinning I (2010) The C Terminus of the Alb3 Membrane Insertase Recruits cpSRP43 to the Thylakoid Membrane. J. Biol. Chem. 285: 5954-5962**

Pubmed: [Author and Title](#)  
CrossRef: [Author and Title](#)  
Google Scholar: [Author Only](#) [Title Only](#) [Author and Title](#)

**Gerdes L, Bals T, Klostermann E, Karl M, Philipp K, Hunken M, Soll J, Schünemann D (2006) A Second Thylakoid Membrane-localized Alb3/Oxal/YidC Homologue Is Involved in Proper Chloroplast Biogenesis in Arabidopsis thaliana. J. Biol. Chem. 281: 16632-16642**

Pubmed: [Author and Title](#)  
CrossRef: [Author and Title](#)  
Google Scholar: [Author Only](#) [Title Only](#) [Author and Title](#)

**Glauert AM (1998) Practical Methods for Electron Microscopy. Portland Press 17: 293**

Pubmed: [Author and Title](#)  
CrossRef: [Author and Title](#)  
Google Scholar: [Author Only](#) [Title Only](#) [Author and Title](#)

**Glick BS, Von Heijne G (1996) Saccharomyces cerevisiae Mitochondria Lack a Bacterial-type Sec Machinery. Protein Sci. 5: 2651-2652**

Pubmed: [Author and Title](#)  
CrossRef: [Author and Title](#)  
Google Scholar: [Author Only](#) [Title Only](#) [Author and Title](#)

**Göhre V, Ossenbühl F, Crèvecoeur M, Eichacker LA, Rochaix JD (2006) One of Two Alb3 Proteins Is Essential for the Assembly of the Photosystems and for Cell Survival in Chlamydomonas. Plant Cell 18: 1454-1466**

Pubmed: [Author and Title](#)  
CrossRef: [Author and Title](#)  
Google Scholar: [Author Only](#) [Title Only](#) [Author and Title](#)

**Gorecka M, Alvarez-Fernandez R, Slattery K, McAusland L, Davey PA, Karpinski S, Lawson T, Mullineaux PM (2014) Absciscic acid signalling determines susceptibility of bundle sheath cells to photoinhibition in high light-exposed Arabidopsis leaves. Philos. Trans. R. Soc. Lond. B Biol. Sci. 369: 20130234**

Pubmed: [Author and Title](#)  
CrossRef: [Author and Title](#)  
Google Scholar: [Author Only](#) [Title Only](#) [Author and Title](#)

**Gouy M, Guindon S, Gascuel O (2010) SeaView Version 4: A Multiplatform Graphical User Interface for Sequence Alignment and Phylogenetic Tree Building. Mol. Biol. Evol. 27: 221-224**

Pubmed: [Author and Title](#)  
CrossRef: [Author and Title](#)  
Google Scholar: [Author Only](#) [Title Only](#) [Author and Title](#)

**Groves MR, Mant A, Kuhn A, Koch J, Dubel S, Robinson C, Sinning I (2001) Functional Characterization of Recombinant Chloroplast Signal Recognition Particle. J. Biol. Chem. 276: 27778-27786**

Pubmed: [Author and Title](#)  
CrossRef: [Author and Title](#)  
Google Scholar: [Author Only](#) [Title Only](#) [Author and Title](#)

**Holsters M, de Waele D, Depicker A, Messens E, van Montagu M, Schell J (1978) Transfection and Transformation of Agrobacterium tumefaciens. Mol. Gen. Genet. 163: 181-187**

Pubmed: [Author and Title](#)  
CrossRef: [Author and Title](#)  
Google Scholar: [Author Only](#) [Title Only](#) [Author and Title](#)

**Hyman S, Jarvis RP (2011) Studying Arabidopsis Chloroplast Structural Organisation Using Transmission Electron Microscopy. Methods Mol. Biol. 774: 113-132**

Pubmed: [Author and Title](#)  
CrossRef: [Author and Title](#)  
Google Scholar: [Author Only](#) [Title Only](#) [Author and Title](#)

**Jakob B, Gamalei Y, Wolf R, Heber U, Gross HJ (1997) Photooxidative Damage in Young Leaves of Declining Grapevine: Does It Result from a New and Possibly Viroid-Related Disease? Plant Cell Physiol. 38: 1-9**

Pubmed: [Author and Title](#)  
CrossRef: [Author and Title](#)  
Google Scholar: [Author Only](#) [Title Only](#) [Author and Title](#)

**Jarvis P, Lopez-Juez E (2013) Biogenesis and Homeostasis of Chloroplasts and Other Plastids. Nat. Rev. Mol. Cell Biol. 14: 787-802**

Pubmed: [Author and Title](#)  
CrossRef: [Author and Title](#)  
Google Scholar: [Author Only](#) [Title Only](#) [Author and Title](#)

**Jia L, Dienhart M, Schramp M, McCauley M, Hell K, Stuart RA (2003) Yeast Oxa1 Interacts with Mitochondrial Ribosomes: the Importance of the C-terminal Region of Oxa1. EMBO J. 22: 6438-6447**

Pubmed: [Author and Title](#)  
CrossRef: [Author and Title](#)  
Google Scholar: [Author Only](#) [Title Only](#) [Author and Title](#)

**Jiang F, Yi L, Moore M, Chen M, Rohl T, Van Wijk KJ, De Gier JW, Henry R, Dalbey RE (2002) Chloroplast YidC Homolog Albino3 Can Functionally Complement the Bacterial YidC Depletion Strain and Promote Membrane Insertion of Both Bacterial and Chloroplast Thylakoid Proteins. J. Biol. Chem. 277: 19281-19288**

Pubmed: [Author and Title](#)  
CrossRef: [Author and Title](#)  
Google Scholar: [Author Only](#) [Title Only](#) [Author and Title](#)

**Jonas-Straube E, Hutin C, Hoffman NE, Schunemann D (2001) Functional Analysis of the Protein-interacting Domains of Chloroplast SRP43. J. Biol. Chem. 276: 24654-24660**

Pubmed: [Author and Title](#)  
CrossRef: [Author and Title](#)  
Google Scholar: [Author Only](#) [Title Only](#) [Author and Title](#)

**Katoh K, Standley DM (2013) MAFFT Multiple Sequence Alignment Software Version 7: Improvements in Performance and Usability. Mol. Biol. Evol. 30: 772-780**

Pubmed: [Author and Title](#)  
CrossRef: [Author and Title](#)  
Google Scholar: [Author Only](#) [Title Only](#) [Author and Title](#)

**Klostermann E, Droste Gen Helling I, Carde JP, Schunemann D (2002) The Thylakoid Membrane Protein ALB3 Associates with the cpSecY-Translocase in Arabidopsis thaliana. Biochem. J. 368: 777-781**

Pubmed: [Author and Title](#)  
CrossRef: [Author and Title](#)  
Google Scholar: [Author Only](#) [Title Only](#) [Author and Title](#)

**Kovacheva S, Bedard J, Patel R, Dudley P, Twell D, Rios G, Koncz C, Jarvis P (2005) In vivo Studies on the Roles of Tic110, Tic40 and Hsp93 During Chloroplast Protein Import. Plant J. 41: 412-428**

Pubmed: [Author and Title](#)  
CrossRef: [Author and Title](#)  
Google Scholar: [Author Only](#) [Title Only](#) [Author and Title](#)

**Kroll D, Meierhoff K, Bechtold N, Kinoshita M, Westphal S, Vothknecht UC, Soll J, Westhoff P (2001) VIPP1, a Nuclear Gene of Arabidopsis thaliana Essential for Thylakoid Membrane Formation. Proc. Natl. Acad. Sci. U. S. A. 98: 4238-4242**

Pubmed: [Author and Title](#)  
CrossRef: [Author and Title](#)  
Google Scholar: [Author Only](#) [Title Only](#) [Author and Title](#)

**Kubis S, Patel R, Combe J, Bedard J, Kovacheva S, Lilley K, Biehl A, Leister D, Rios G, Koncz C, Jarvis P (2004) Functional Specialization Amongst the Arabidopsis Toc159 Family of Chloroplast Protein Import Receptors. Plant Cell 16: 2059-2077**

Pubmed: [Author and Title](#)  
CrossRef: [Author and Title](#)  
Google Scholar: [Author Only](#) [Title Only](#) [Author and Title](#)

**Lee LY, Fang MJ, Kuang LY, Gelvin SB (2008) Vectors for multi-color bimolecular fluorescence complementation to investigate protein-protein interactions in living plant cells. Plant Methods 4: 24**

Pubmed: [Author and Title](#)  
CrossRef: [Author and Title](#)  
Google Scholar: [Author Only](#) [Title Only](#) [Author and Title](#)

**Liu C, Willmund F, Golecki JR, Cacace S, Hess B, Markert C, Schroda M (2007) The Chloroplast HSP70B-CDJ2-CGE1 Chaperones Catalyse Assembly and Disassembly of VIPP1 Oligomers in Chlamydomonas. Plant J. 50: 265-277**

Pubmed: [Author and Title](#)  
CrossRef: [Author and Title](#)  
Google Scholar: [Author Only](#) [Title Only](#) [Author and Title](#)

**Long D, Martin M, Sundberg E, Swinburne J, Puangsomlee P, Coupland G (1993) The Maize Transposable Element System Ac/Ds as a Mutagen in Arabidopsis: Identification of an Albino Mutation Induced by Ds Insertion. Proc. Natl. Acad. Sci. U. S. A. 90: 10370-10374**

Pubmed: [Author and Title](#)  
CrossRef: [Author and Title](#)  
Google Scholar: [Author Only](#) [Title Only](#) [Author and Title](#)

**Moore M, Goforth RL, Mori H, Henry R (2003) Functional Interaction of Chloroplast SRP/FtsY with the ALB3 Translocase in Thylakoids: Substrate Not Required. J. Cell Biol. 162: 1245-1254**

Pubmed: [Author and Title](#)  
CrossRef: [Author and Title](#)  
Google Scholar: [Author Only](#) [Title Only](#) [Author and Title](#)

**Moore M, Harrison MS, Peterson EC, Henry R (2000) Chloroplast Oxa1p Homolog Albino3 Is Required for Post-translational Integration of the Light Harvesting Chlorophyll-binding Protein into Thylakoid Membranes. J. Biol. Chem. 275: 1529-1532**

Pubmed: [Author and Title](#)  
CrossRef: [Author and Title](#)  
Google Scholar: [Author Only](#) [Title Only](#) [Author and Title](#)

**Mori H, Summer EJ, Ma X, Cline K (1999) Component Specificity for the Thylakoidal Sec and Delta pH-dependent Protein Transport Pathways. J. Cell Biol. 146: 45-56**

Pubmed: [Author and Title](#)  
CrossRef: [Author and Title](#)  
Google Scholar: [Author Only](#) [Title Only](#) [Author and Title](#)

**Ossenbuhl F, Gohre V, Meurer J, Krieger-Liszkay A, Rochaix JD, Eichacker LA (2004) Efficient Assembly of Photosystem II in Chlamydomonas reinhardtii Requires Alb3.1p, a Homolog of Arabidopsis ALBINO3. Plant Cell 16: 1790-1800**

Pubmed: [Author and Title](#)  
CrossRef: [Author and Title](#)  
Google Scholar: [Author Only](#) [Title Only](#) [Author and Title](#)

**Pasch JC, Nickelsen J, Schunemann D (2005) The Yeast Split-ubiquitin System to Study Chloroplast Membrane Protein Interactions. Appl. Microbiol. Biotechnol. 69: 440-447**

Pubmed: [Author and Title](#)  
CrossRef: [Author and Title](#)  
Google Scholar: [Author Only](#) [Title Only](#) [Author and Title](#)

**Rambaut A, Drummond AJ (2007) Tracer v1.4.**

**Ronquist F, Teslenko M, van der Mark P, Ayres DL, Darling A, Hohna S, Larget B, Liu L, Suchard MA, Huelsenbeck JP (2012) MrBayes 3.2: Efficient Bayesian Phylogenetic Inference and Model Choice Across a Large Model Space. Syst. Biol. 61: 539-542**

Pubmed: [Author and Title](#)  
CrossRef: [Author and Title](#)  
Google Scholar: [Author Only](#) [Title Only](#) [Author and Title](#)

**Saller MJ, Wu ZC, de Keyser J, Driessen AJ (2012) The YidC/Oxa1/Alb3 Protein Family: Common Principles and Distinct Features. Biol. Chem. 393: 1279-1290**

Pubmed: [Author and Title](#)  
CrossRef: [Author and Title](#)  
Google Scholar: [Author Only](#) [Title Only](#) [Author and Title](#)

**Spence E, Bailey S, Nenninger A, Moller SG, Robinson C (2004) A Homolog of Albino3/Oxa1 Is Essential for Thylakoid Biogenesis in the Cyanobacterium Synechocystis sp. PCC6803. J. Biol. Chem. 279: 55792-55800**

Pubmed: [Author and Title](#)  
CrossRef: [Author and Title](#)  
Google Scholar: [Author Only](#) [Title Only](#) [Author and Title](#)

**Stengel KF, Holdermann I, Cain P, Robinson C, Wild K, Sinning I (2008) Structural Basis for Specific Substrate Recognition by the Chloroplast Signal Recognition Particle Protein cpSRP43. Science 321: 253-256**

Pubmed: [Author and Title](#)  
CrossRef: [Author and Title](#)  
Google Scholar: [Author Only](#) [Title Only](#) [Author and Title](#)

**Sundberg E, Slagter JG, Fridborg I, Cleary SP, Robinson C, Coupland G (1997) ALBINO3, an Arabidopsis Nuclear Gene Essential for Chloroplast Differentiation, Encodes a Chloroplast Protein that Shows Homology to Proteins Present in Bacterial Membranes and Yeast Mitochondria. Plant Cell 9: 717-730**

Pubmed: [Author and Title](#)  
CrossRef: [Author and Title](#)  
Google Scholar: [Author Only](#) [Title Only](#) [Author and Title](#)

**Szyrach G, Ott M, Bonnefoy N, Neupert W, Herrmann JM (2003) Ribosome Binding to the Oxa1 Complex Facilitates Co-translational Protein Insertion in Mitochondria. EMBO J. 22: 6448-6457**

Pubmed: [Author and Title](#)  
CrossRef: [Author and Title](#)  
Google Scholar: [Author Only](#) [Title Only](#) [Author and Title](#)

**Tu CJ, Peterson EC, Henry R, Hoffman NE (2000) The L18 Domain of Light-harvesting Chlorophyll Proteins Binds to Chloroplast Signal Recognition Particle 43. J. Biol. Chem. 275: 13187-13190**

Pubmed: [Author and Title](#)  
CrossRef: [Author and Title](#)  
Google Scholar: [Author Only](#) [Title Only](#) [Author and Title](#)

**Tu CJ, Schuenemann D, Hoffman NE (1999) Chloroplast FtsY, Chloroplast Signal Recognition Particle, and GTP Are Required to Reconstitute the Soluble Phase of Light-harvesting Chlorophyll Protein Transport into Thylakoid Membranes. J. Biol. Chem. 274: 27219-27224**

Pubmed: [Author and Title](#)  
CrossRef: [Author and Title](#)  
Google Scholar: [Author Only](#) [Title Only](#) [Author and Title](#)

**Woolhead CA, Thompson SJ, Moore M, Tissier C, Mant A, Rodger A, Henry R, Robinson C (2001) Distinct Albino3-dependent and -**

**independent Pathways for Thylakoid Membrane Protein Insertion. J. Biol. Chem. 276: 40841-40846**

Pubmed: [Author and Title](#)

CrossRef: [Author and Title](#)

Google Scholar: [Author Only](#) [Title Only](#) [Author and Title](#)

**Wu FH, Shen SC, Lee LY, Lee SH, Chan MT, Lin CS (2009) Tape-Arabidopsis Sandwich - a Simpler Arabidopsis Protoplast Isolation Method. Plant Methods 5: 16**

Pubmed: [Author and Title](#)

CrossRef: [Author and Title](#)

Google Scholar: [Author Only](#) [Title Only](#) [Author and Title](#)

**Zhang L, Aro EM (2002) Synthesis, Membrane Insertion and Assembly of the Chloroplast-encoded D1 Protein into Photosystem II. FEBS Lett. 512: 13-18**

Pubmed: [Author and Title](#)

CrossRef: [Author and Title](#)

Google Scholar: [Author Only](#) [Title Only](#) [Author and Title](#)

**Zhang YJ, Tian HF, Wen JF (2009) The Evolution of YidC/Oxa/Alb3 Family in the Three Domains of Life: A Phylogenomic Analysis. BMC Evol. Biol. 9: 137**

Pubmed: [Author and Title](#)

CrossRef: [Author and Title](#)

Google Scholar: [Author Only](#) [Title Only](#) [Author and Title](#)

**Zuppini A, Gerotto C, Moscatiello R, Bergantino E, Baldan B (2009) Chlorella saccharophila Cytochrome f and its Involvement in the Heat Shock Response. J. Exp. Bot. 60: 4189-4200**

Pubmed: [Author and Title](#)

CrossRef: [Author and Title](#)

Google Scholar: [Author Only](#) [Title Only](#) [Author and Title](#)